UiT The Arctic University of Norway

Faculty of Health Sciences - Department of Medical Biology

The Regulatory Relationship between E2F4 and MiRNA-363, and it's Relevance to Oral Cancer

Geed Alaa Assadi

Master's thesis in Biomedicine - MBI-3911- June 2020

TABLE OF CONTENTS

ACKNOWLEDGEMENTS

This thesis was supported by The Tumor Biology Research Group and The Department of Medical Biology, Faculty of Health Sciences, University of Tromsø, Norway in the period from August 2019 to May 2020.

First and foremost, I would like to express my sincere appreciation to my supervisor *Associate professor Qalbi Khan* for the excellent supervision, guidance, unlimited patience and encouragement throughout the process of researching and thesis writing.

I would like to thank everyone from the research group at the Department of Medical Biology, Faculty of Health Sciences for the positive environment and gradience, with special thanks to *Bente Mortensen (Senior Engineer), Marit Seppola (Senior Engineer), Cuong Khuu, (Senior Engineer and Researcher), Manyahilishal Etana Kitaw (Lab Engineer), and Beate Hegge (Senior Engineer)* for their invaluable advice, guidance and assistance in performing, understanding and analyzing the laboratory trials.

My appreciation also extends to my beloved friends for their unceasing love and support through the stress and the hardest of times, that energized me to keep going.

Finally, I would like to express my profound love and gratitude to my family for their boundless love, unfailing support and continuous encouragement throughout my years of study and through the process of researching and writing this thesis. This achievement would not have been possible without my mother *(Wegdan Hasha),* father *(Alaa Assadi)* and my brothers *(Ahmed and Faisal)*. Thank you.

Thank you,

Tromsø, August 2020
Geed Alaa Assadi

ABBREVIATIONS AND ACRONYMS

3'-UTR	Three prime untranslated region
5' UTR	Five prime untranslated region
Ab	Antibody
Cdks	Cyclin Dependent Kinases
cDNA	Complementary DNA
CPS-3	Chemiluminescence Peroxidase Substrate-3
CLL	Chronic Lymphocytic Leukemia
CO_2	Carbon dioxide
DAB	3,3'-Diaminobenzidine
DP	Dimerization Partner transcription factors
DTT	Dithiothreitol
DMEM	Dulbecco's Modified Eagle's Medium
DMSO	Dimethyl Sulfoxide
DNA	Deoxyribonucleic Acid
E2F	E2F transcription factor
E2F4	E2F transcription factor 4
FBS	Fetal Bovine Serum
FFPE	Formalin-Fixed, Paraffin-Embedded
G0 phase	G note phase/resting phase
G1 phase	Gap 1 phase
gDNA	Genomic DNA
GS	Goat Serum
GTC buffer	Guanidine Thiocyanate buffer
HIER	Hear-Induced Epitope Retrieval/Heat-Mediated Antigen Retrieval

HNC	Head and Neck Cancer
HNSCC	Head and Neck Squamous-Cell Carcinoma
HPV	Human papillomavirus
HRP	Horseradish Peroxidase
IgG	Immunoglobulin G
IHC	Immunohistochemistry
ISH	In Situ Hybridization
kDa	Kilodalton
mA	Milliampere
miRNA-363	hsa-miR-363-5p (CGGGTGGATCACGATGCAATTT)
miRNA	MicroRNA/Micro-Ribonucleic Acid
mRNA	Messenger RNA/Messenger Ribonucleic Acid
NAC	No Amplification Control
ncRNA	Noncoding RNA/Noncoding Ribonucleic Acid
nt	Nucleotide
OE	Oral Epithelium
OSCC	Oral Squamous-Cell Carcinoma
p53	Tumor protein p53/Tumor suppressor p53/Photoprotein p53
PBS	Phosphate-Buffered Saline
PCR	Polymerase Chain Reaction
pH	Pondus Hydrogenii
pRb/Rb	Retinoblastoma protein
pre-miRNA	Precursor MicroRNA/Precursor Micro-Ribonucleic Acid
pri-miRNA	Primary MicroRNA/Primary Micro-Ribonucleic Acid
PVDF membrane	Polyvinylidene fluoride membrane

RIPA buffer	Radioimmunoprecipitation Assay buffer
RISC	RNA-induced silencing complex
RNA	Ribonucleic Acid
Rpm	Revolutions per minute
RT	Room Temperature
RT-qPCR	Reverse-Transcriptase Quantitative Polymerase Chain Reaction
SCC	Squamous Cell Carcinoma
SDS	Sodium Dodecyl Sulphate
SDS-PAGE	Sodium Dodecyl Sulphate Polyacrylamide Gel Electrophoresis
S phase	Synthesis phase
siRNA	Small interfering RNA/Small interfering Ribonucleic Acid
ssRNA	Single stranded RNA/Single stranded Ribonucleic Acid
TBS	Tris Buffered Saline
TBST	Tris Buffered Saline and 0.1% Tween-20
TMA	Tissue Micro Array
UT-SCC-24A	University of Turku – Squamous Cell Carcinoma – 24A
UT-SCC-24B	University of Turku – Squamous Cell Carcinoma – 24B
UV	Ultraviolet
V	Volt
WB	Western Blot

ABSTRACT

BACKGROUND

Oral Squamous Cell Carcinoma (OSCC) is the most common type of head and neck cancer and persists a leading cause of cancer associated mortality and morbidity universally. Survival rate is still poor at less than 50% urging the need for biomarkers to allow better diagnosis, prognosis and therapeutic strategies. In this study we focus on E2F4, a repressor of cell cycle, and further propose its regulatory relationship with MiRNA-363.

METHODS

Western blot (WB) was used to measure E2F4 protein expression and RT-qPCR was used to measure relative gene expression of *E2F4*, in UT-SSC-24A against UT-SCC-24B. Immunohistochemistry (IHC) of human tongue tissues was also applied to detect location and expression pattern of E2F4. Furthermore, transient transfection of the cell lines with miRNA-363 was applied to detect changes in E2F4 protein and gene expression.

RESULTS

E2F4 gene expression did not show major differences in the two cell lines. However, the protein levels did show difference both in the whole cell lysates and in the cytoplasmic fractions of cell lines. The IHC study revealed a relatively higher expression in cytoplasm of the cells belonging to the invasive front and areas with budding. Nearly 50% cell number decrease was observed in UT-SCC-24B, as a result of transfection with miRNA-363. This effect was not observed for UT-SCC-24A. A decrease of E2F4 protein levels in transfected UT-SCC-24B cells was further demonstrated by WB. Similar effect was observed in a immunoblot of transfected cytoplasmic fraction, but not observed for the nuclear fraction. Lastly, downregulation of *E2F4* gene expression was exhibited by the transfected UT-SCC-24B cells with miRNA-363.

CONCLUSION

Our data indicate the involvement of E2F4 and miRNA-363 in OSCC and show a regulatory relationship between them. Furthermore, due to the findings of E2F4's dynamic expression pattern, this study also proposes E2F4 as a potential biomarker for OSCC.

1 INTRODUCTION

1.1 HEAD AND NECK SQUAMOUS CELL CARCINOMA

Cancers are usually classified by the cell and tissue type from which the tumor originates. The class of cancers emerging from epithelial cells are called carcinomas, and constitute about 80% of all cancers (1, 2). This high incident rate is owed to the proliferative nature of epithelial tissues and their exposure to various forms of physical and chemical damage that promote oncogenesis (1). Some epithelia are specialized for protection. Tumors stemming from the protective epithelial layer are typically recognized as squamous cell carcinomas (SCCs). More than 90% of all head and neck cancers (HNCs), including all oral cancers, arise from SCCs and are generally referred to as head and neck squamous cell carcinoma (HNSCC) (2-6). HNCs are among the top ten most common cancers in the world, and accounts for the majority of HNSCCs; encompassing tumors of the oral cavity, pharynx, larynx, nasal cavity, salivary glands and the oral cavity (5, 7, 8).

1.1.1 ORAL SQUAMOUS CELL CARCINOMA

Oral cancers from SCC, also referred to as oral squamous cell carcinoma (OSCC), is a malignant neoplasia which includes tumors of the buccal mucosa, retromolar triangle, gingiva, tongue, floor of the mouth, and mucosal surface of the lip (4, 9). Globally, OSCC is the 6th most prevalent type of cancer and has been observed more frequently in men than women (4, 9, 10). There are more than 600,000 new cases of oral cancer reported annually, with mortality above 300,000 deaths per annum (4, 6, 11, 12). Moreover, in most published articles, the five-year survival rate for OSCC is still poor at less than 50%. This poor survival rate has been linked to late screening, with about 60% - 80% of patients presenting with large lesions at the time of diagnosis. Also, OSCC has high rates of recurrence and metastasis (6, 12-14).

1.1.2 RISK FACTORS, TREATMENT AND PREVENTION

The major risk factors for OSCC include exposure to cancer-causing agents, mostly tobacco smoking and alcohol consumption. Other risk factors may include ultraviolet (UV) radiations, genetic predispositions and often infection with human papillomavirus (HPV), which is linked to cancers arising from the oropharynx (4, 5, 10, 14). Depending on the stage, the treatment of

OSCC is typically multimodal, and comprises surgical intervention in combination with radiation therapy and/or chemotherapy.

Preventative and management methods include screening programs, a healthy lifestyle, avoidance of high-risk habits, and the development of specific biomarkers. A large number of cases of oral cancer are diagnosed at an advanced stage, which is linked to poor prognosis, local recurrence and metastasis. Hence an earlier diagnosis would benefit a better prognosis for the patients (4, 6, 13-15). Consequently, this provokes the need to better understand the molecular pathology of oral cancers and underline the lack and need for biomarkers as prognostic tools, which could aid in better detection and diagnosis, and creating appropriate targeted therapies. However, very few biomarkers have showed clear clinical application potential (4, 12, 15-17). This calls for a focus on, not only research for novel OSCC biomarkers, but also their molecular relationship with other molecules and proteins that may complement them, thereby strengthening the reliability of the "biomarker set". Such studies may entail protein to protein interaction, RNA to RNA- or, as ours, protein to miRNAs interaction.

1.2 MICRORNA

miRNAs are one of the three main classes of small noncoding RNAs, which are highly conserved and about 22 nucleotides long single-stranded RNAs (ssRNAs). More than 2000 distinctive miRNAs have been recognized within the human genome up to date. Additionally, its presumed that about more than 50% of protein-coding genes acquires regulation via miRNAs (18-22). A series of modern findings have shown that the noncoding part of RNA are way more prevalent and of great functional significance for normal development, physiology, and in disease than previously assumed. In fact, the most interesting and broadly studied sub-class of noncoding RNAs (ncRNAs) are microRNAs (miRNAs) (1, 2, 18, 23).

1.2.1 BIOGENESIS, FUNCTION AND REGULATION

miRNAs are synthesized from DNA via transcription by RNA polymerase II into primary miRNAs (pri-miRNAs) which are then processed into precursor miRNAs (pre-miRNAs) and mature miRNAs. Recently, the biogenesis of miRNA has been divided into non-canonical and canonical pathways with the latter being the dominant pathway by which miRNAs are processed. The biogenesis starts with a pri-miRNA being transcribed from DNA, which forms a double-stranded RNA hairpin by self-complementarity of its nucleotide sequences.

Following, nuclear cleavage occurs by excision of a small segment of the pri-miRNA via the microprocessor complex (protein complex involving Drosha), forming the pre-miRNA. Once precursor miRNA is formed, it is exported to the cytoplasm for further cleavage and processing by the Dicer enzyme; creating a double-stranded miRNA that's about 22 nt long. Ultimately, a single strand mature miRNA is assimilated into an RNA-induced silencing complex (RISC) to act as a guide targeting specific mRNAs in the cytoplasm through base-pairing. The degree of base-pairing, extensive or less extensive, determines the fate of the target mRNA resulting in either its degradation or translational inhibition, respectively (Fig. 1) (1, 2, 19-22).

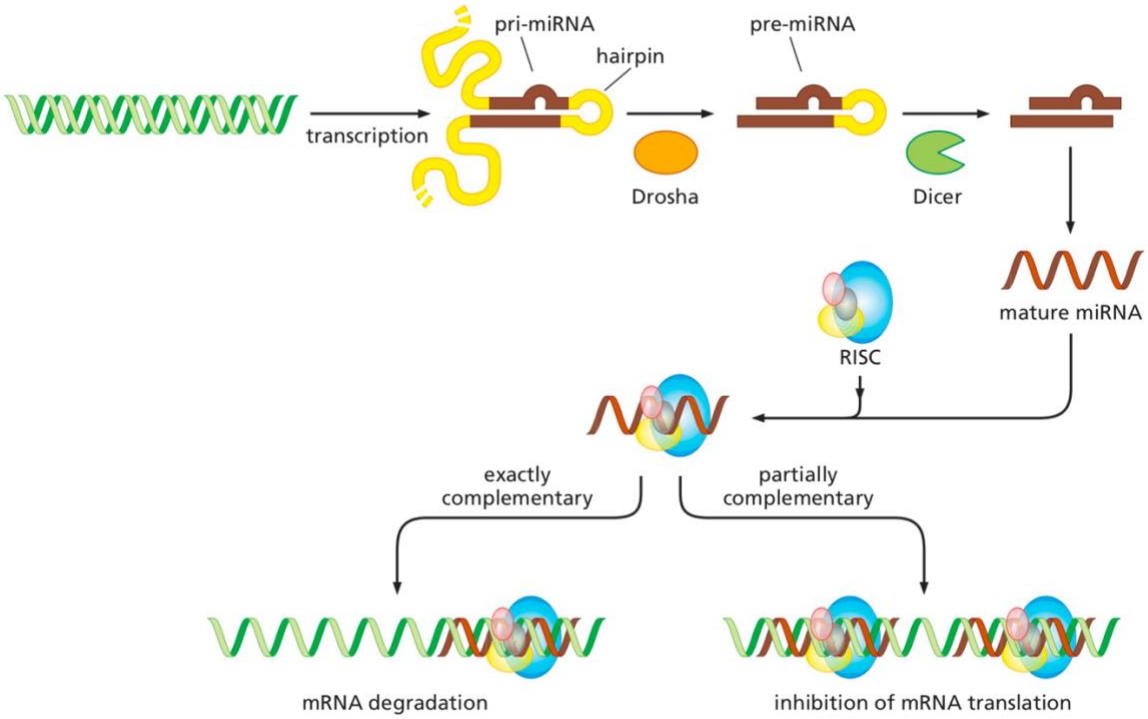

Figure 1: miRNA biogenesis and gene regulation. *The canonical pathway of miRNA synthesis in a cell starts with transcription of miRNA genes by RNA polymerase II resulting in a pri-miRNA that's enzymatically cleaved by Drosha-proteins complex into pre-miRNA in the nucleus. The pre-miRNA hairpin structure is transported to the cytoplasm where it is cleaved by the Dicer enzyme into about 22 nt miRNA duplex. The double-stranded miRNA is unwounded, one of the strands is degraded while the other binds to the miRNA-induced silencing complex (RISC) to target mRNAs in the cytoplasm inducing gene regulation depending on the degree complementarity of the miRNA/mRNA complex (2).*

The predominant function of miRNAs is post-transcriptional gene silencing, where its estimated that the translation of over 50% of protein-coding genes is regulated by miRNAs. This is shown to occur via the miRNAs interaction with the three prime untranslated regions (3' UTR) of target mRNAs in the cytoplasm, resulting in mRNA degradation or translational repression (Fig. 1) (18, 20, 22-24). However, recent studies have shown various other interactions of miRNAs with other regions including the 5' UTR, coding sequences, and gene

promoters. The binding to 5' UTR and coding regions is suggested to have silencing effects on gene expression whereas interaction with the promoter region has been reported to induce either transcriptional activation or transcriptional suppression. Furthermore, more recent studies have revealed that a fair percentage of miRNAs shuttle between nucleus and cytoplasm, indicating to their functionality in regulating gene expression at both the transcriptional and translational level in the cell (20, 21, 24, 25). Moreover, miRNAs play important role in regulation of development and numerous physiological processes such cell growth, proliferation, differentiation, apoptosis, metabolism, defense and homeostasis (18, 20, 23-25).

miRNA regulation is chiefly determined by their location factor. About 50% of the all known miRNAs are considered intragenic, located within protein-coding or non-coding genes. Whereas, the remaining miRNAs are intergenic, located between genes (20, 22, 26). Naturally, miRNAs synthesis is mainly regulated at transcriptional level by a network of transcription factors that either repress or promote the expression of miRNAs. However, miRNAs can also be regulated at post-transcriptional level, during processing, during modifications and during decreased miRNA stability (19, 27).

1.2.2 ROLE IN CANCER

Numerous miRNAs have been observed in human cancer pathogenesis by either upregulating or downregulating various critical steps involved in cancer development. Thus, the dysregulation of miRNA expression may play a crucial role in the initiation, progression, and metastasis of cancer. This irregularity can occur by means of epigenetic and/or genetic alterations, influencing the making of the primary miRNAs, their processing to mature miRNAs and/or interactions with target mRNAs (2, 18, 24, 25). The first indication for the link between miRNAs and tumor development was reported in 2002 in chronic lymphocytic leukemia (CLL), where aberrant expression of miR-15/16 as a result of chromosome 13q14 deletion was demonstrated. Many studies have also shown that miRNAs can behave as oncogenes (onco-miRs) promoting tumorigenesis, proliferation, angiogenesis, invasion and migration; or as tumor suppressors (TS-miRs) controlling the cell cycle, apoptosis, differentiation, DNA repair, angiogenesis, and metastasis. miR-155, miR-372, miR-21, miR-4260, miR-363 and the miR-17-92 family have been reported to serve as oncomiRs in many cancer types such as human glioblastomas, lymphomas, breast cancer, colorectal cancer, lung cancer, pancreas and prostate cancers. Conversely, Let-7, miR-200c and miR-34 were reported to be regularly downregulated/tsmiRs in lung cancer, glioma and many other cancers (18, 19, 21-23, 25, 26,

28). Furthermore, recent studies have shown a number of miRNAs that also may be interesting in OSCCs (28-30).

1.2.3 MiRNA as a Biomarker in Diagnostic, Prognostic and Therapeutics in Cancer – OSCCs

Many studies have shown that the expression of miRNAs is tissue-specific as well as diseases-specific. Accordingly, suggesting that distinct miRNA expression signatures can be used to typify specific tissue and disease states including subtypes of normal and malignant tissues (19, 21, 23). In addition, miRNAs have been found in numerous studies to be released into extracellular fluids, including blood, plasma, serum, urine, saliva, cystic fluid, pancreatic juice, and sputum. These circulating miRNA are rather stable in bodily fluids and function as signaling molecules to mediate cell-cell communications; where their aberrant expression levels have been linked with multiple diseases including several types of cancer (20-23, 25). These findings facilitate the use of miRNA as biomarkers in the diagnosis, prognosis and potential treatment of cancer; which have been demonstrated in many studies for example: miR-125a and miR-200a levels in saliva or miR-184 and miR-378 overexpression in OSCC tissue can be used for oral cancer diagnosis and prognosis (19-23, 25, 30). Similar to miR-184 and miR-378 that were observed to as act oncogenes in OSCC, miR-26a, miR-26b, miR-497, miR506 and miR-363 were observed to as act suppressors in OSCCs (28-30). Moreover, comprehensive understanding of nuclear miRNA, its function and dysregulation has urging potential to its applications in a number of clinical settings in the future (24, 31).

As aforementioned, numerous miRNAs can promote tumor development by disrupting essential cell cycle regulators. On the other hand, studies have also indicated that miRNAs function in combination with transcriptional factors involved in the regulation of cell cycle such as, c-Myc, E2F or p53. Both scenarios illustrate the regulatory role of miRNAs in cell cycle control and hence their relevance in cancer (19, 22, 32).

1.3 The Role of Cell Cycle in Carcinogenesis

Cancer involves many different diseases caused by a common mechanism that is uncontrolled cell division or cell growth. Clinically, malignant tumors are indicated by three main features including uncontrolled growth, invasion and metastasis. These features distinguish malignant tumors from benign tumors, which are self-limited, non-invasive and non-metastatic. From a

pathogenetic point of view, cancers are considered to be sporadic and hereditary, accounting for over 95% and less than 5% of human cancers, respectively (2, 33-36). A single mutation is not adequate to cause cancer as the model currently guiding our thinking about carcinogenesis is the multistep model. Thus, the development of cancer may be divided into at least three stages: initiation, promotion, and progression (Fig. 2). In this model, carcinogenesis is proposed to be an accumulation of cell mutations encompassing both the activation and inactivation of oncogenes and tumor suppressor genes, respectively (2, 9, 37, 38).

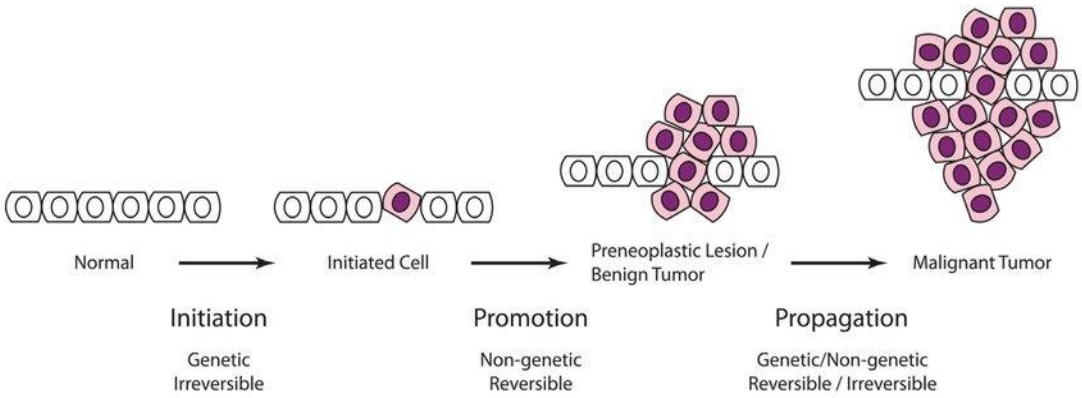

Figure 2: The multistep model of carcinogenesis. *Initiation is the first step of carcinogenesis which is a result of mutation where a permanent or irreversible genetic change occur. Promotion is the second step in cancer development which involve the stimulation or acceleration of tumor progression without any genetic mutations. Progression is last step in carcinogenesis and is characterized by genomic instability and malignancy (39).*

Proto-oncogenes are normal genes engaged with positive regulation of the cell cycle and cell proliferation, where a gain-of-function mutation or retroviral modifications can convert them into overactive or overexpressed cancer-promoting genes that are usually known as oncogenes (e.g. Ras, Myc and Her-2/Neu). On the other hand, tumor suppressors, p53 and Rb, are genes that negatively regulate the cell cycle in which a loss-of-function mutation or epigenetic silencing of genes can lead to their malfunction or inactivation hence promoting cancer development (1, 2, 37). The impairment of tumor suppressor genes arises rather more frequently during tumorigenesis than the activation of proto-oncogenes into oncogenes, such that the p53 gene is mutated in more than 50% of all cases of cancer and the inactivation of the Rb pathway occurs in most human cancers. This denotes to how vital these genes are in protecting us against cancer and to how crucial is the loss of genetic information in the development of most if not all human cancers. Notwithstanding numerous of these critical genes being identified, the basic number and characteristics of molecular modifications that distinguish tumor growth are still not elucidated. Nonetheless, mutations may induce cancer directly by causing cells to proliferate when they shouldn't or indirectly by causing genetic or epigenetic instability and so

speeding the occurrence of other inherited changes that will directly stimulate tumor growth (1, 2, 37, 40). Finally, tumor cells acquire distinctive capabilities during the course of their development which are known by the hallmarks/characteristics of cancer (2, 9, 41).

Genes that encode proteins needed for cell cycle progression, entry into the S phase and DNA replication, are commonly regulated by the E2F family of transcription factors. It's a large family of transcription factors consisting of nine members, which are all key determinants in the G1/S transition of the cell cycle, cell proliferation and apoptosis following intra- and extra-cellular signals (42-45).

1.3.1 CELL CYCLE REGULATION

Cell cycle control involves the major processes of the cell cycle, namely DNA replication, mitosis and cytokinesis. This is achieved through intracellular signaling by Cyclin Dependent Kinases (Cdks), Cyclins, p53 and Retinoblastoma Protein (pRb/Rb); and extracellular signaling through Mitogens, Growth Factors and Survival Factors. Such intracellular molecules can either positively regulate the cell cycle allowing its progression (e.g. Cdks and cyclins) or negatively regulate the cell cycle leading to its arrest (e.g. p53 and Rb) (1, 2, 46, 47).

The regulation of the levels of these proteins is a central concern in understanding cell cycle control and its dysregulation in human disease. Genetic changes of one or more regulatory proteins of the cell cycle, causing its malfunctioning, overexpression or absence, can lead to uncontrolled cell division and ultimately tumorigenesis. This indicates how proper control of the protein levels of these regulators is vital for cell growth, division and survival (1, 2, 32, 46, 47).

Recent evidence has revealed that a number of miRNAs may be involved in regulating the cell cycle, which is done by controlling the protein levels of several cell cycle regulators. Evidently, the dysregulation of such miRNAs may stimulate cancer by varying the protein levels of critical onco- or tumor suppressor genes (32, 48, 49).

1.3.2 E2F TRANSCRIPTION FACTORS – E2F4

The nine members of the E2F protein family are subdivided based on sequence conservation, structure and function, into canonical activators (E2F1-3A/B), canonical repressors (E2F4-6), and atypical repressors (E2F7-8). E2F4-6 have the major roles in the induction of cell cycle

exit, differentiation and in negative regulation of G0/G1 transition of the cell cycle, respectively. Both canonical repressors and activators carry out their transcriptional regulation by binding target promoter sequences through a single DNA-binding domain with a member of the dimerization partner (DP) family of proteins. While, the atypical repressors are understood to bind target sequences through two DNA-binding domains independent of the DP proteins for transcriptional regulation (44, 50-55).

The activity and expression of the E2F protein family are closely regulated at several levels, including transcription, mRNA stability, post-translational modifications, interaction with regulatory proteins and protein stability (52, 55). One of the most known control mechanisms is via interactions with the pRb and the pRb-related proteins p107 and p130, which are also known as the pocket proteins. E2F1-3A/B specifically bind to pRb for regulation, while E2F4 can bind to all the Rb proteins but is primarily regulated by p107 and p130, and E2F5 binds mainly to p130. In *vivo*, E2F4 and E2F5 are thought to be regulated in a different way compared to the activating E2F members (42, 52, 54).

As aforementioned, the pRb is a tumor suppressor protein that bind to E2F halting cell cycle progression into the S phase. Upon mitogenic stimuli, the activity of cyclin D-Cdk4/6 (G1-Cdk) and cyclin E-Cdk2 (G1/S-Cdk) complexes increases, triggering the phosphorylation of Rb family proteins. This inactivates the Rb, promoting the dissociation of the repressive Rb/E2F complexes, activating E2Fs and leads to the E2F-dependent transcription of target genes required for cell cycle progression (Fig. 3) (32, 42, 43, 52).

E2F4 is the most abundant E2F-family member and is constitutively expressed throughout the cell cycle unlike other E2Fs, accounting for the majority of the total E2F in most cells. Its critical activity is to maintain cell cycle arrest in G0/G1 phases in association with members of the Rb protein family. The repressive E2F4/Rb family complexes are replaced by free activating E2Fs as the cells enter the S phase (Fig. 3) (42, 54, 55).

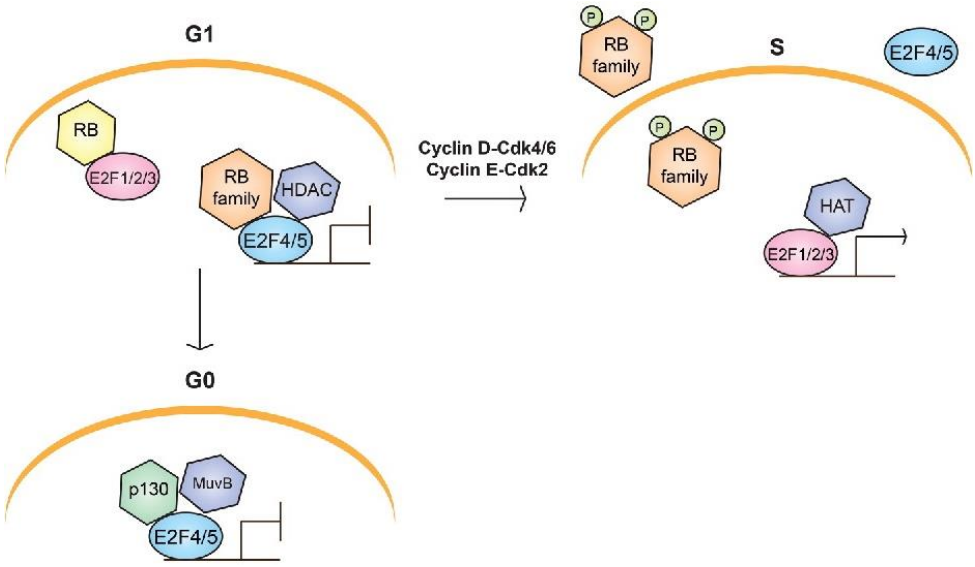

Figure 3: The Rb/E2F pathway. *Entry into the S phase upregulate Cyclin-CDK activity leading to phosphorylation of the RB family proteins. This promotes the dissociation of repressive RB/E2F complexes, releasing "activator" E2Fs to stimulate the expression of genes required for cell cycle progression (42).*

Furthermore, E2F4 is thought to lack a nuclear localization signal and is dependent on the Rb proteins for its nuclear translocation and cytoplasmic sequestration. E2F4 is reported to be nuclear in quiescent cells (G0 and early G1 phases) and cytoplasmic in cycling cells, indicating the importance of regulation of its nuclear-cytoplasmic shuttling in cell cycle (42, 55, 56). However, only little is explored about E2F4 shuttling machinery in cell cycle regulation, and therefore the localization of the protein could/should be interesting to study.

In cancers, E2F4 tends predominantly to function as an oncogene which is more linked to its non-canonical role in pro-proliferative cells than with its canonical, repressive role in the cell cycle. Many human tumors including, prostate, breast, and head and neck cancers, have been reported to have high E2F4 protein expression, which has been correlated with poor prognosis (42, 57, 58).

1.4 AIM AND RATIONALE OF THE STUDY

Cancer remains one of the most feared, controversial and challenging diseases yet to be diagnosed, and is a leading cause of death globally in both, less and the more economically developed countries (1, 2, 59). Among these, Oral squamous cell carcinoma (OSCC) remains one of the cancer types that is associated with the most severe disease- and treatment related morbidity. The survival rate is low and unchanged for the past three decades, and the side effects of the treatment are often devastating for the quality of life. An urgent and an increased focus on OSCC, its disease development, better diagnosis and treatment is therefore warranted (4, 12, 60).

The overall purpose of the study is:

To explore and report novel bio-molecular insight that contribute to the current understanding of OSCC and its treatment.

The specific aim of the study is:

Evaluate a specific transcription factor of interest, E2F4, for clinical value in treatment, diagnosis and prognosis of OSCC by studying

- E2F4's gene expression in the human oral cancer cell lines, UT-SCC-24A and UT-SCC-24B.
- E2F4's sub-cellular protein expression in the human oral cancer cell lines, UT-SCC-24A and UT-SCC-24B.
- the regulatory effects, if any, of miRNA-363 on E2F4 in the human oral cancer cell lines, UT-SCC-24A and UT-SCC-24B.
- location of E2F4 in OSCC-sections.

Technical approaches used achieve the aims:

- Cell culturing and Transient transfection of oral cancer cell lines.
- Western blot and Real-time Quantitative Reverse Transcription Polymerase Chain Reaction of cultured and transfected oral cancer cell lines
- Immunohistochemistry of human oral cancer tissues
- Spectrophotometry, Light and Virtual Slide Microscopy, and Digital imaging of blots.

2 MATERIALS AND METHODS

A list with details of all materials, antibodies, buffers and primers used to execute the different experimentations in this study, is provided in the appendix.

2.1 CELL CULTURE

Cell culture is one of the major techniques used in molecular and cellular biology, where cells are obtained directly from normal or unhealthy tissues, a primary culture, or a cell line. Cell culturing is carried out under strict laboratory settings of sterility and a controlled physiochemical environment, which is done to mimic the *in vivo* environment successfully allowing the cells to survive and proliferate (61). All cell culture protocols were performed following the right aseptic techniques and working in a laminar flow hood.

2.1.1 DECONTAMINATION

A major potential pitfall in a cell culture lab is contamination. This can be in the form of chemical contamination from media or equipment, biological contamination from bacteria or yeast, or even cross-contamination from a different strain of cells. Hence, decontamination and cleaning ensure that materials, environmental surfaces or instruments are safe to handle. All of the materials, including the laminar flow hood, were disinfected with 70% alcohol before usage. Pre-sterilized cell culture flasks, glass pipettes and falcon tubes were provided. Disposable pipettes, pipette boy, pipettor and pre-sterilized pipette tips were used.

2.1.2 CELL LINES AND REAGENTS

Head and neck squamous cell carcinoma cell lines UT-SCC-24A and UT-SCC-24B were established from clinical squamous cell carcinoma samples of oral tissue by Turku University Hospital, Finland. UT-SCC-24A arise from a primary tongue squamous cell carcinoma, while UT-SCC-24B were metastases from a tongue squamous cell carcinoma derived from neck. Both were achieved from the same 41 years old male patient (62). All cell lines were cultured in Dulbecco's Modified Eagle's Medium (DMEM) supplemented with 10% Fetal Bovine Serum (FBS) (Table 1, Appendix I), and all reagents including the medium was warmed up to about 37°C at least 30 min before use.

2.1.3 THAWING FROZEN CELLS

Frozen cells immersed in liquid nitrogen were thawed by working carefully and quickly to ensure high percentage of cell survival, as the thawing procedure is usually stressful to frozen cells. The outside of the vial was wiped with 70% ethanol and the vial was then placed in the sterile hood and left to thaw at room temperature (RT). The desired amount of pre-warmed growth medium, 10 mL, was placed into a 15 mL flacon tube in which the thawed cells were transferred to. The cell suspension in the falcon tube was thereafter centrifuged at approximately 200-1200 rpm for 5-10 min (the actual centrifugation speed and duration varies depending on the cell type). The clarity of the supernatant and visibility of a whole pellet was examined, and the supernatant was discarded carefully without disrupting the pellet. This was to remove toxic Dimethyl Sulfoxide (DMSO) (Table 1, Appendix I) from the cells before culturing, which is frequently used during cryopreservation to reduce crystallization during freezing.

Following DMSO removal, the cells were resuspended gently in 5 mL pre-warmed growth medium and transferred into the appropriate/desired culture flask. Initially, a T25 flask was often selected in order to allow rapid cell-to-cell contact and consequently allow the cells to proliferate faster. An appropriate amount of medium was subsequently added to the flask and they were left to incubate in humidified atmosphere of 5% CO_2 at 37°C. The cells usually reached about 80-90% confluency by day three (Fig. 4). The cells were visualized under an inverted microscope (Leica DM IRB - Leica Microsystems, Wetzlar, Germany) after 1-1.5 days to ensure survival and attachment to the flask, as well as to control if the medium needed to be changed.

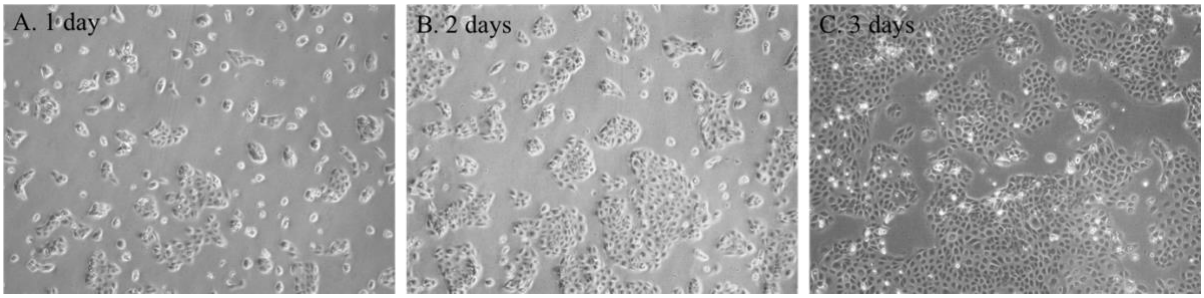

Figure 4: Phase contrast images of healthy UT-SCC-24A cells at varying confluency. *The culture was started in a T25 culture flask in 10% FBS DMEM medium and grown in an incubator with humidified atmosphere of 5% CO2 at 37°C. A) Showing the cells at 10-20% confluency after 24hrs/1 day of seeding. B) Showing the cells at 40-50% confluency after 48hrs/2 days of seeding. C) Showing the cells at 80-90% confluency after 72hrs/3 days of seeding.*

2.1.4 SUB-CULTURING OR SPLITTING OF CELLS

As the cells reached approximately 80% confluency, they would require sub-culturing and passaging (splitting). This was done to keep the cells at optimal density for continued growth and to stimulate further proliferation. The process of splitting adherent cells involves transferring a small number of the cells from a previous culture into a new flask with fresh growth media, using Trypsin/EDTA (Table 1, Appendix I). Trypsin is a proteolytic enzyme which breaks down proteins and is used to dissociate strongly adherent cells from the culture flask in which they were being cultured (63).

Splitting was carried out by decanting the spent medium from the culture flask of the desired cell line carefully using a pre-sterile glass pipette to avoid contamination and changing the glass pipette used when removing media from a culture flask with another cell line to avoid cross-contamination. Following medium removal, the culture flask was gently washed with 1xPhosphate-Buffered Saline (1xPBS) (Table 2, Appendix II) by adding a suitable amount (usually 10 mL for a T75 culture flask and about 5 mL for a T25 culture flask) to the opposite side of the attached cell layer to avoid disturbing the cell layer, and by shaking the flask back and forth few times. The washing solution was then discarded, and the washing step was repeated at least twice to ensure that the flask is clean from any traces of culture media that may inhibit the action of trypsin and ensure removal of dead cells (64, 65). Normally, 2mL of trypsin was added to detach the adhered cells, the flask was gently shaken to get complete coverage of the cell layer and the cells were left to incubate for 2-10 min in 5% CO_2 at 37^{o}C. However, the amount of trypsin to be added and the time of incubation required for trypsin to work may vary with the cell line used. Therefore, to avoid over-trypsinization, as the toxicity of trypsin can severely damage the cells (63), cells were observed every few minutes under the microscope for detachment. Some mechanical force can be/was used to accelerate cell detachment by tapping the flask a few times.

Once the cells have detached, pre-wared culture media of 4 mL was added to the flask immediately. This was done to inactivate the trypsin. At this point, the required volume of cells from the cell suspension at the required split ratio was transferred into a new flask. The new flask was then filled up with culture media to the appropriate volume (e.g. total volume in a T25 flask of approximately 3-5 mL, in a T75 flask of approximately 8-15 mL, in a T175 flask of approximately 15-35 mL). Lastly, the flask was left to incubate in 5% CO_2 at 37°C for one day or more depending on the split ratio, giving rise to a different passage of the cell line. The

cell lines were split at varying ratios depending on whether the cells should be prepared for an experiment on a specific day or should just be kept running for future use or as a backup. In this case, when splitting a healthy UT-SCC-24A cell line from a confluent flask (80-90%) at a ratio of 1:2, it reached confluency (80-90%) in about two days when grown in the same size culture flask (T75). Meanwhile, when splitting a confluent healthy UT-SCC-24B cell line at a ratio of 1:4, it required about 3 days to reach confluency again, grown in the same size culture flask (T75). To obtain optimal seeding density, splitting of cells for two days in row and more than a 1:10 ratio was avoided.

2.1.5 FREEZING CELLS OR CRYOPRESERVATION

Cryopreservation is the process by which very low temperatures are used to preserve structurally intact living cells and tissues (66). Maintaining a properly frozen cell stock is a very vital element of cell culturing. This is because cells in a running cell culture tend to experience undesirable outcomes such as genetic variations, senescence, microbial contamination, and even sometimes equipment failure, which can be very costly and time consuming to replace. Thus, it is important to cryopreserve an established cell line for long-term storage and later usage.

The freezing of the adherent cell lines usually started with detachment of the cells from their culture flask by the process of trypsinization, described in the 'Sub-culturing or Splitting of Cells' section above. The desired amount of freezing medium/cryoprotectant was prepared in a pre-sterilized flacon tube, before starting the trypsinization procedure, consisting of 10% DMSO and 90% FBS (e.g. 2 mL of freezing media was prepared by mixing 0.2 mL of DMSO with 1.8 mL FBS). Freezing medium reduces crystallization (formation of ice crystal during freezing), which can injure cells and cause cell death. It also facilitates the entry process of organic molecules into tissues at low toxicity (66). Once trypsinization was stopped, the desired number of cells to be frozen was calculated with the required volume of freezing medium. The suspended cells in the culture flask was transferred into a falcon tube,15 mL, and centrifuged for about 5 mins at 200-1200 rpm. The supernatant was suctioned out carefully without disrupting the cell pellet. The pellet was thereafter resuspended in cold freezing medium and the cell suspension was aliquoted into cryogenic vials/cryovials labelled with cell line name, date, passage number, and person's initials. Cells were frequently and gently mixed while aliquoting to keep a homogeneous cell suspension. Lastly, the cryovials were immediately

moved into a styrofoam holder and placed in a freezer at -70°C. The frozen cells could then be transferred to liquid nitrogen tank for indefinite stability and longer storage.

2.1.6 COUNTING OF THE CELLS WITH COUNTESS II

Accurate and precise measurements of the number of cells and their viability is another very important element of cell culturing, allowing reproducible and better analysis. Automated cell counting is usually more favored than manual counting due to its higher accuracy, simplified workflow and the amount of time saved. The dye exclusion method was applied to determine the number of viable cells present in the cultured cells. This method is based on the principle that live cells possess intact cell membranes that exclude certain dyes, such as trypan blue, whereas dead cells do not, hence it allows us to test for cell viability easily. One of the most commonly used dyes is Trypan Blue (Table 1, Appendix I). It was used at a concentration of 0.4%, which was the correct concentration for use on the Countess II FL Automated Cell Counter machine (Table 1, Appendix I).

The initial and most important part of cell counting process is sample preparation which was achieved by firstly detaching the cells following the same procedure described under the 'Sub-culturing or Splitting of Cells' section. Once the cells had been resuspended in the medium and the cell suspension was homogenously mixed by gentle vortexing or by manually flicking the flask/tube, a small amount (about 0.5-1 mL) of the cell suspension was taken-out from the flask and placed in a 1.5 mL Eppendorf tube. Following, 198 µL of the cell suspension from the Eppendorf tube was transferred into another 1.5 mL Eppendorf tube with 2 µL of 0.4% Trypan Blue and mixed gently by flicking the tube. This was done as the uptake of Trypan Blue varies from cell type to cell type, where higher concentration of it results in higher false dead cell number. Using a pipette, 10 µL of the cell mixture was removed and applied into the well of a disposable Countess chamber slides (Table 1, Appendix I) allowing capillary action to draw it inside. The chamber slide was then inserted into the Countess II FL Automated Cell Counter machine and the number of viable/living cells (calculated by the machine) was noted down for further applications and/or analysis. Cell counting was done three to four times to ensure accurate cell counting results.

2.2 WESTERN BLOT

One of the most frequently used methods in protein analysis is Western blotting (WB), which is based on transferring (blotting) proteins separated based on molecular weight by gel electrophoresis, to a membrane. This is followed by detection of the protein of interest using specific antibodies and a chemiluminescent substrate. WB can provide qualitative and semi-quantitative information about a specific protein by detecting the specific protein from a pool of proteins extracted from cell lysates or tissues (67-69). Western blot was performed using lysates from different cellular fractions of the cell lines UT-SCC-24A and UT-SCC-24B using primary antibody for E2F4.

2.2.1 SAMPLE PREPARATION – CELL LYSIS AND PROTEIN MEASUREMENT

Cells were seeded to achieve about 2.0 x 10_6 cells overnight and subsequently harvested by trypsinization. A cell count was done to ensure that the correct amount of cells was harvested. The cell suspension was then moved from the culture flask into a conical/falcon tube and centrifuged for about 5-10 mins at 200-1200 rpm. The supernatant was aspirated without disrupting the pellet and PBS was added. This was done to wash the cells with PBS prior to resuspension in a microcentrifuge tube. All work from this point onward was carried out on ice.

Cell lysis for proteins extraction and solubilization was carried out using different lysis buffers depending on the localization of the protein of interest in the cells. The cell suspension in PBS was centrifuged in a microcentrifuge for about 5 min at 1500 rpm at 4°C and the supernatant was discarded without disrupting the pellet. Preparing a whole cell lysate for about two million cells was done by adding 200 µL of radioimmunoprecipitation assay lysis buffer (RIPA buffer) (Table 2, Appendix II) containing protease inhibitor (1:100) (Table 1, Appendix I) to the microcentrifuge tube with the dry pellet. The protease inhibitor was added to prevent denaturation or degradation of the proteins in the cell lysate. Following, the microcentrifuge tube was sonicated before protein measurement to ensure successful cell lysis. Nuclear and cytoplasmic fractions of the cell were prepared by using the NE-PER Nuclear and Cytoplasmic Extraction Reagents kit (Table 1, Appendix I) according to the manufacturer's protocol.

The protein concentration of the samples was determined and measured by the DC Protein Assay Kit (Table 1, Appendix I) using the VERSAmax PLUS spectrophotometer (Table 1, Appendix I) where the unknown protein concentration was compared to known samples. This

is an important step prior to gel electrophoresis, as it allows the loading of a specific amount of protein on the gel, thus enabling comparison between the samples. The protein measurement was carried out according the protocol provided by the kit. PBS was used to make the standard and the samples were usually diluted in PBS (1:10)), depending on the concentration of the sample.

2.2.2 GEL ELECTROPHORESIS

The same protein concentration in a desired volume (fitting for the gel well size) was prepared in Eppendorf tubes and loaded in each well. Using the same volume for all samples will give fewer pipetting errors. The samples were diluted in 5x loading buffer (Table 2, Appendix II) to increase their density to easily sink to the bottom of the wells of the gel and to become negatively charged by their attachment to sodium dodecyl sulphate (SDS) anions to be separated during sodium dodecyl sulphate polyacrylamide gel electrophoresis (SDS-PAGE) according to their size only and not core electrical charge. The samples were also mixed with 1 µL of 3M Dithiothreitol (DTT) (Table 1, Appendix I) which is a reducing agent and was used for disruption of protein disulfide bonds in electrophoresis.

The Biotinylated Protein Ladder (Table 1, Appendix I) was also diluted in 1xloading buffer (diluted in Milli-Q water) and mixed with 1 µL of 3M DTT and SeeBlue Pre-Stained Protein (Table, Appendix I) Standard as tracking dye to easily visualize the movement of proteins during electrophoresis and western transfer efficiency. The prepared samples including the ladder were boiled at 100˚C for about 5-10 minutes and mixed by vortexing before and after the heating step for best outcome. Heat was applied to the samples to denature the 3D structure of the proteins to enable access to the antibody, and also help in maintaining the negative charge from neutralization to allow the protein to move in the electric field supplied during electrophoresis.

600 mL of 1xNuPAGE MES SDS running buffer (Table 2, Appendix II) and used to rinse off the ready-made gel before inserting it into the electrophoresis apparatus. Both the loading buffer and the gel running buffer contain SDS to allow the separation of proteins to be solely by size/molecular weight and not by electric charge. Post loading of the samples and the ladder prepared into the gel wells, the electrophoresis apparatus was filled with gel running buffer, and the gel was run at 200V (125 mA) for 35 minutes. Using very high voltage was avoided as it can overheat the gel which perhaps damage/deform the bands.

2.2.3 BLOTTING TO MEMBRANE

Blotting/transfer buffer (Table 2, Appendix II) was prepared and one sheet of polyvinylidene fluoride (PDVF) membrane (Table 1, Appendix I) was cut along with two Whatman filter papers fit to the dimension of the gel. A mark was made on the membrane recognize the top from the bottom side of the membrane by cutting one of the top or bottom corners. The membrane was prepared by wetting in methanol bath for 15 seconds, rinsing in water bath for about 1 min and placing in blotting buffer for about 5 minutes or longer until the gel is retrieved and ready for transfer. Once electrophoresis is done, the gel is retrieved by opening the gel cassette and removing the bottom edge and the comb of the gel. The filter papers along with sponges were wetted in the blotting/transfer buffer. The blotting sandwich was built in the following order: 2-3 sponges, 1 Whatman paper, the gel, the membrane, 1 Whatman paper, and 2-3 sponges; avoiding and removing any air bubbles as they can disrupt the transfer of protein to the membrane and squeezing out extra liquid. Following, the blotting sandwich was held firmly and placed in the apparatus (Table 1, Appendix I) and tightened with the clamp to ensure a tight contact between gel and membrane. The inner chamber of device was filled with transfer buffer and the outer chamber was filled with cold water for cooling. The blot was run at 30V (170 mA) for 1 hour.

2.2.4 IMMUNOBLOTTING - BLOCKING AND ANTIBODY STAINING

After blotting, blocking of the membrane was carried out using 5% milk in 1xTBST (Tris Buffered Saline and 0.1% Tween-20) (Table 2, Appendix II) for 1 hour at RT. This was done to prevents nonspecific binding of the antibodies to the membrane. All incubations were conducted with membrane placed in a 50 mL falcon tube with gentle agitation on a rotator. After blocking, the membrane was incubated with primary antibody (Ab), Anti-E2F4 antibody (Table 3, Appendix III), in blocking buffer (1:1000) overnight at 4°C. Following the primary Ab removal, the membrane was washed three times with 1xTBST for 3-5 min per wash. The membrane was then incubated with secondary antibody (Anti rabbit, made in goat, HRP-labelled, Table 3, Appendix III) in blocking buffer (1:5000) for 1 hour at RT; and then washed twice with 1xTBST and once with 1xTBS for 3-5 min per wash.

2.2.5 DETECTION, IMAGING AND STORAGE

Detection was carried out using Chemiluminescence Peroxidase Substrate-3 (CPS-3) kit (Table 1, Appendix I). The substrate was made by mixing the detection reagents in one to one ratio (1:1) from the kit in a 50 mL falcon tube (mixtures of 20 mL in total). The falcon tube was covered with aluminum foil and was left to incubate for at least 30 min before use. The membrane was then placed in a bath of the substrate for about 5-10 mins in a dark room before placing into the LAS-4000 imaging machine (Table 1, Appendix I). The membrane was placed between plastic sheet removing any bubbles and placed into the machine in the right position for imaging.

The membrane was stored for further applications or downstream analysis by sealing it between plastic sheets with a small amount of 1xTBST and storing at 4°C in a fridge for short term storage or in a freezer at -20°C for longer storage time.

2.2.6 LOADING CONTROL AND SEMI-QUANTITATIVE ANALYSIS

Loading control was performed using two polyclonal antibodies, Anti-Vinculin and Anti-Lamin B1, for the whole cell, cytoplasmic and nuclear fractions of the cell lines UT-SCC-24A and 24B, respectively. Equal protein loading was verified using the loading controls vinculin and lamin B1 for their respective cellular fraction specificity (70, 71). Probing of the membrane with loading control antibodies was done following the same procedure under the "Immunoblotting - Blocking and Antibody Staining" section. However, Vinculin primary Ab was used at a concentration of 1:400 while Lamin B1 at 1:5000, in 5% milk blocking buffer.

Semi-quantitative/densitometric analysis of the Western blot was carried out using the software Image Studio Lite by Licor company. The loading control densitometric values were used as reference point for data normalization.

2.3 TRANSFECTION

Transfection is the process by which foreign nucleic acid is introduced into mammalian cells via reagent/chemical, instrument/physical or virus/biological-based methods. The exogenous nucleic acid introduced can either be stably or transiently transfected. This powerful process aims primarily to study the function of genes or expression of proteins, by turning on or off specific gene expression in cells, and to produce recombinant proteins (2, 72). Evaluation of

the transfection efficiencies was carried out by Cuong Khuu PhD, Department of Oral Biology, University of Oslo. More than 95% of the cells were transfected when using INTERFERin (Table 1, Appendix I) as transfection reagent. Moreover, the negative control (AllStars scrambled) has been tested and validated to exhibit minimal off target effect with mRNA microarrays for several cell lines according to the manufacturer Qiagen.

2.3.1 SEEDING CELLS – DAY1

For day one of transfection 25 x 10^5 cells per T25 flask were seeded from each cell line, UT-SCC-24A and 24B, in 10% FBS culturing media and left to incubate overnight in 5% CO_2 at 37^oC.

2.3.2 TRANSIENT LIPID-BASED TRANSFECTION PROCEDURE – DAY2 TO DAY4

In transient transfection, the exogenous nucleic acid exists in the host cell for only a short period of time, usually between 24 - 72 hours, and is not integrated into the host genome. Lipid-based transfection method is applied by the majority of the available transfection reagents, which generally contain lipid that form liposomes in an aqueous environment. Accordingly, transfection occur when DNA/RNA and liposome interact spontaneously to form a Lipid-DNA complex, which enter the host cell by fusing with the plasma membrane.

Following overnight incubation of the seeded cells, a 10 nM transfection mixture (4.8 µL RNA of 10 µM stock, 16 µL INTERFERin and 800 µL DMEM incubate for 15-20 minutes at RT) of miR-363-5p (Table 1, Appendix I) or Allstars scrambled control (Table 1, Appendix I) or transfection reagent only (Mock) was added to 4 mL 5% FBS culturing media without antibiotic. The cells were visualized under the microscope, pictured at three different marked areas per flask and left to incubate overnight in 5% CO2 at 37^oC.

On day three the transfection media was removed from the flask and replaced with 10% FBS culturing media. Cells were visualized under the microscope, pictured at the same marked areas per flask and left to incubate overnight in 5% CO_2 at 37^oC. Following, the cells were checked and pictured after 48 hours and left to incubate overnight.

2.3.3 HARVESTING CELLS – DAY5

After 72 hours of incubation, the transfected cells were checked and pictured using the microscope. The cells were then harvested and prepared for cell count, WB and RT-qPCR following the same procedure under section 2.2.1.

2.4 QUANTITATIVE REVERSE TRANSCRIPTION POLYMERASE CHAIN REACTION

Quantitative Reverse Transcription Polymerase Chain Reaction (RT-qPCR) is a widely used method in research, medicine, molecular biology and many other fields to amplify a segment of DNA starting from RNA. Its characterized as a direct and easy procedure with high sensitivity and specificity for RNA detection, classification and quantification. This method is based on a DNA replication using a thermal cycler, thermostable polymerase, primers (with which one can select what part of the DNA to amplify) and free nucleotides. Each cycle is about 1 min and produce double amount of DNA (2^n for amount of DNA per n cycles). Regularly, isolated RNA is first mixed with reverse transcriptase, random hexamers, polydT primers and nucleotides forming a cDNA (complementary DNA) strand complementary to the RNA strand. The cDNA is then used as a template for standard qPCR, where a thermostable polymerase is used to amplify the DNA/cDNA through denaturation, annealing and elongation. These steps are temperature dependent and are executed in a thermocycler. Unlike standard qPCR, dye-based qPCR allows the collection of data as the reaction progresses, by the measuring the generated fluorescent signal each cycle. The fluorescent signal increases proportionally to the amount of PCR product, hence the RNA/DNA is quantified in “real time” and such process is called real-time qPCR.

2.4.1 RNA EXTRACTION AND QUANTIFICATION

Cells were seeded and harvested as described under section 1.2.1. Cell lysis for RNA extraction was carried out using 350 µL lysis buffer containing 1 mL denaturing guanidine thiocyanate (GTC) buffer from the E.Z.N.A. HP Total RNA Kit (Table 1, Appendix I) and 13.3 µL 3M DTT. Following, the RNA isolation was carried out using the E.Z.N.A. HP Total RNA Kit according to the protocol provided with the kit. The RNA concentration in the samples was then measured using the Nanodrop 2000 spectrophotometer (Table I, Appendix I) and noted for downstream applications.

2.4.2 GENOMIC DNA WIPEOUT AND CDNA SYNTHESIS

Genomic DNA (gDNA) removal was carried to avoid any false positive in the final PCR as a result of residual gDNA in the isolated RNA samples. The RNA samples were thawed on ice and were gently mixed by pipetting or exposing to a short duration of heat (e.g. 2 min at 37^{o}C) before use. Template RNA samples were diluted with nuclease-free water to contain 100-200 ng total RNA. Both the gDNA wipeout and the cDNA synthesis were carried out using the QuantiTect Reverse Transcription Kit (Table 1, Appendix I), following the manufacturer's recommendations. The resulting cDNA samples were diluted in nuclease-free water (1:10) prior to storage at -20^{o}C. A no amplification control (NAC) was prepared for three random RNA samples. NAC was used to exclude the RNA polymerase from the cDNA reaction to verify the absence of gDNA. Such control is very important when employing a SYBR-Green probe.

2.4.3 REAL-TIME QPCR

Prior real time PCR, the 1:10 diluted template samples were thawed and further diluted in nuclease-free water to 1:30 dilution. 8 µL of each 1:30 diluted sample was mixed with a master mix containing 10 µL 1x FastStart Essential DNA Green Master (Table 1, Appendix I), 0.6 µL forward primer (10 µM, Table 4, Appendix IV), 0.6 µL reverse primer (10 µM, Table 4, Appendix IV), and 0.8 µL nuclease-free water; making a total of 20 µL for each well of the 96-well qPCR plate. Accordingly, the qPCR was performed in duplicates or triplicates using the LightCycler 96 instrument (Table 1, Appendix I). The target cDNA in the samples was amplified through 40 cycles, in a series of 600 seconds preincubation at 95^{o}C, 10 seconds two step amplification at 95^{o}C and 1 min at 60^{o}C to evaluate the relative expression of the selected genes (Table 4, Appendix IV).

Non-template control (NTC) were included in each run to verify the absence of carry-over contamination. Melting curves were included in each PCR run to verify amplification of a single PCR product. Such analysis is very important when working with SYBR Green probe as it binds to any double-stranded DNA product and lacks sequence specificity.

2.4.4 STANDARD CURVE AND DOUBLE-DELTA CT ANALYSIS

Standard curve analysis was applied to test the qPCR amplification efficiency of the primers used in this study. This was done by relative quantification where the quantity of each

experimental sample is first established using a standard curve which is later expressed relative to a calibrator sample. Standard curves were generated separately for the gene of interest and each housekeeping/reference gene. Seven two-fold serial dilutions of cDNA template known to express the gene of interest in high abundance was performed using the above-mentioned PCR program. In a base-10 semi-logarithmic graph, the threshold cycle (C_T) was plotted versus the dilution factor to fit the data in a straight line and the correlation coefficient (R2) for the qPCR efficiency was calculated (Table 4, Appendix IV).

The $\Delta\Delta C_T$ analysis was applied to calculate the relative amount of target mRNA gene normalized against the geometric mean of three reference genes (73). The overall results were presented as average amount of the relative target mRNA gene comparing two different oral cancer cell lines (±standard error of mean).

2.5 IMMUNOHISTOCHEMISTRY

Immunohistochemistry (IHC) is a procedure that uses the principle of the specific antibody-antigen binding in biological tissues for visualizing cellular components in tissue samples. It is a very useful tool as it allows detection for existence, distribution and localization of specific cellular components (such as proteins) in different cell types, biological states, and/or subcellular localization within complex tissues. IHC is commonly used in research and clinical laboratories where molecules of interest are investigated, using different IHC-based methods that depends on cell type specificity and sensitivity, to study their functions in both healthy and diseased cells and tissues on a molecular, cellular or tissue level. It also plays a vital role in cancer diagnostics and is used in the diagnosis of 11–38% of all carcinoma cases. Furthermore, an IHC procedure encompasses many crucial stages, including proper handling of the sample, appropriate fixation and blocking, antigen retrieval, selection and preparation of antibody and reagents, incubation, washing, and counterstaining (74-77).

2.5.1 SAMPLE PREPARATION

Three whole tissue sections of 4 μm thickness of formalin-fixed, paraffin-embedded (FFPE) tongue tissues from three different oral cancer/OSCC patients, were used for immunohistochemistry analysis. The sections belong to a cohort-study on OSCC at the Tumor Biology Research Group at the Arctic University of Norway. Additional information, such as

concerning tissue handling and preparations, storage and ethical considerations, is accessible in already published studies (78, 79).

2.5.2 DEPARAFFINIZATION AND REHYDRATION

Prior to the deparaffinization and rehydration procedure the sections were dried overnight at 60°C. The section slides were then placed in a rack and initially deparaffinized in a xylene bath for 10 mins at room temperature (RT). This was repeated again using a second fresh xylene bath. Xylene treatment was performed under a hood, as xylene is a flammable, toxic, and volatile organic solvent. Complete removal of paraffin in FFPE sections prior to staining was very important, as its presence can obscure target antigens and its hydrophobic property can lead to poor staining of the sections. Following, the slides were rehydrated in graded ethanol baths for 5 mins per bath at RT, starting with two baths in 100% ethanol and two baths in 96% ethanol. Finally, the slides were washed/placed in water for about 3-5 mins to wash off ethanol. To avoid non-specific antibody binding that will consequently lead to high background staining, drying out of the sections was prevented from this point onwards (slides may remain in water until the next step).

2.5.3 HEAT-MEDIATED ANTIGEN RETRIEVAL OR HEAT-INDUCED EPITOPE RETRIEVAL

Unlike deparaffinization which is always required prior to staining, antigen or epitope retrieval is actually not. Formalin or other aldehyde fixation tend to create methylene bridges that cross-link proteins covalently masking antigenic sites and inhibiting antibody binding. This results in weak or false negative immunostaining detection of certain proteins, which is where antigenic retrieval treatment is required to unmask the antigenic sites and allow antibody binding for enhanced immunostaining. Heat-Mediated Antigen Retrieval or Heat-Induced Epitope Retrieval (HIER) is most commonly used technique for antigen retrieval which can be performed using a pressure cooker, a microwave, or a vegetable steamer with an appropriate buffer (75, 76).

HIER antigenic retrieval of the FFPE tongue tissue sections was performed using a domestic microwave and the Tris-EDTA buffer (10 mM Tris Base, 1 mM EDTA solution, 0.05% Tween 20, pH 9.0). The buffer at the right pH, 9.0, was placed in a microwaveable beaker. The deparaffinized slides from the water bath were placed into the beaker and into the microwave.

The microwave was set to full power, waited until the solution was boiling and left the sample at 100°C for 20 min. Following, the beaker was taken out of the microwave and left to incubate for 20 min at RT. The antigen retrieved slides were then washed/placed under running de-ionized water (Milli-Q water) for about 10 min at RT.

2.5.4 BLOCKING OF ENDOGENOUS PEROXIDASE ACTIVITY

The blocking of endogenous peroxidase activity in the tissue samples was performed by first taking the samples out of the water bath and drying by wiping around the section gently with sterile gauze/tissue paper. The slides were thereafter placed in a wet-chamber to avoid dryness and finally blocked with diluted 3% hydrogen peroxide (DAKO EnVision+ System-HPR Kit, Table 1, Appendix I). A 10 mL working solution of 0.3% hydrogen peroxide was made and used for the blocking by mixing 1 mL of 3% hydrogen peroxide with 9 mL Milli-Q water. This was done as certain tissues, cells and/or antigens can be damaged by high concentration of hydrogen peroxide. The sections were left to incubate for 10 min at RT. Blocking of endogenous peroxidase activity is very crucial in the detection step, as it will prevent false positive detection and high background staining. After blocking, the sections are washed with Milli-Q water following a series of three washes with 1xPBS for 5 min per wash at RT.

2.5.5 BLOCKING OF NONSPECIFIC SITES

The blocking of nonspecific sites was carried using 1.5% Goat Serum (Table I, Appendix I) as a blocking reagent, to prevent non-specific binding of the Fc portion of primary and/or secondary antibodies during immunostaining, as well as to reduce undesirable background staining during detection. A 1000 µL of 1.5% Goat serum (GS) blocking buffer was prepared by mixing 15 µL GS with 985 µL 1xPBS. The sections were gently dried with sterile gauze/tissue paper and placed in a wet-chamber/humidified chamber. About 250 µL of the blocking buffer was added to each tissue sections, making sure to cover the entire tissue, and left to process for 20 minutes at RT. Here, the blocking solution was removed by simply draining the slides for a few seconds and wiping around the sections with sterile gauze/tissue paper. Washing was skipped as the antibodies will be diluted in the blocking buffer.

2.5.6 IMMUNOSTAINING USING INDIRECT METHOD

Immunostaining was carried out using the indirect detection method as it amplifies the detection signal. The primary Ab used was rabbit monoclonal Anti-E2F4 antibody (Table 3, Appendix III), with reactivity to human. The enzyme-conjugated secondary Ab used was anti-rabbit IgG horseradish peroxidase (HRP) (Table 3, Appendix III) Both antibodies were diluted in the 1.5% GS blocking buffer which help in stabilizing the antibodies, promoting their uniform and complete dispersion into the sample and prevent nonspecific binding. About 2 mL of blocking buffer was made by mixing 30 µL of 1.5% GS with 1970 µL 1xPBS. The primary Ab was diluted in blocking buffer 1:250 (i.e. 1 µL of primary Ab was mixed with 250 µL blocking buffer). The desired amount of primary antibody for the three sections was thus prepared by mixing 3 µL of the primary Ab with 750 µL blocking buffer. Following, 250 µL of the primary Ab in blocking buffer was added onto each section and was left to incubate for 30 minutes at RT. All incubations were carried out in a wet-chamber to avoid drying of the tissue sections. After incubation with primary Ab, the sections were washed in Milli-Q water following a series of three washes in 1xPBS for 5 min per wash at RT. After gently drying the sections, 250 µL of the secondary Ab (1:5000) in blocking buffer was added onto each one and they were left to process for 30 minutes at RT. The sections were washed with Milli-Q water following a series of three washes with 1xPBS for 5 min per wash at RT.

The IHC visualization of antibody binding using chromogenic detection is based on a marker such as an enzyme that is conjugated to primary or secondary antibodies. When this enzyme-conjugated antibody is incubated with the appropriate substrates, the enzyme activity leads to the formation of colored precipitate at the antigen localization site; where the detection of a target can be direct involving one antibody or indirect involving a primary and secondary antibody (75, 76). The chromogenic, precipitating substrate used for the HPR (enzyme)-conjugated secondary Ab was Diaminobenzidine (DAB), which results in brown to black color precipitate. The DAB solution was made by adding 1-2 drops of DAB in 1 mL DAB-buffer from the kit ((DAKO EnVision+ System-HPR Kit, Table 1, Appendix I). Washed and dried slides placed in a humidified chamber were covered by 1-2 drops of the DAB solution per section and left to incubate for 10 min at RT. The slides were then washed three times with Milli-Q water for 5 min/wash at RT.

2.5.7 COUNTER STAINING AND MOUNTING

Following immunostaining, counterstaining was carried out to make the morphological structure of cells and tissues well defined and provide contrast to the primary stain for better visualization and detection of the target protein in the cell/tissue under the microscope. The counterstaining reagent used was hematoxylin, which is a basic dye that binds acidic structures of the cell/tissue, mostly nucleic acids of the cell nucleus, resulting in a purplish-blue stained nucleus. The hematoxylin was filtered using a funnel through Whatman's filter paper in a conical flask before usage to remove the metallic sheen surface that all hematoxylins usually form upon standing, which can cause precipitate on the stained sections (77, 80). The slides were stained in filtered hematoxylin for 30 seconds at RT and then rinsed off in running water until the water becomes clear. The slides were then placed in Scott's solution for 15 seconds then washed again with water. Scott's solution is a bluing reagent making the slides bluer via a pH dependent reaction that changes the reddish-purple hematoxylin to a purple blue color.

After counterstaining, the dehydration of the sections was carried out by immersing the slides in a series of baths starting with two baths of 96% ethanol, two baths of 100% ethanol and finally two baths of xylene, all done at RT under the hood for 10 seconds per bath. Finally, the sections were sealed for preservation by mounting with coverslips to prevent section damage, using DPX Mountant (Table 1, Appendix I) for stabilization of the tissue section and the stain.

2.5.8 CONTROLS

Positive tissue controls using palatinal tonsillar where strong staining of the lymphoid areas was observed, hence served as positive control (81). Another positive control for E2F4 using human placental tissue was also done. Negative tissue controls on liver and placental tissue, where the primary antibody was omitted, showed no staining, indicating absence of non-specific binding of the secondary antibody (82). All sections for both positive and negative control were treated according to the same staining protocol as described in the IHC method. Furthermore, other published studies have also demonstrated the reliability of the antibody in similar studies of the protein (83-85)

The primary and secondary antibody specificities have also been evaluated previously as the at the Tumor Biology lab at the Arctic University of Norway for immunofluorescence studies, for the same oral carcinoma cell lines (results not shown). Samples incubated with only secondary

Ab without the primary Ab, showed no staining, revealing lack of nonspecific binding of the secondary Ab to cellular components.

2.5.9 SAMPLE VISUALIZATION AND ANALYSIS

Once the sections are prepared, they were scanned by the Olympus VS120 Virtual Slide Microscope (Table 1, Appendix I) for high-details, enhanced imaging and rapid scanning facilities. Acquisition of images was made via the Olympus Net Image Server (NIS) SQL database software. The images were adjusted with Adobe Photoshop and Microsoft Word/PowerPoint software.

3 RESULTS

3.1 E2F4 EXPRESSION VARIES SIGNIFICANTLY BETWEEN THE CELL LINES UT-SCC-24A AND UT-SCC-24B

E2F4 bands were detected using the LAS-4000 Imaging System at about 50-60 kDa (Fig. 5A, C and E). UT-SSC-24A, trails were ran parallel and are comparable to UT-SSC-24B. The band intensity values for E2F4 were collected from the Image Studio Lite software, corrected for the corresponding loading control and are represented in the bar charts below (Fig. 5B, D and F).

Figure 5B shows about **0,2%** change in band intensity value for E2F4 in the whole cell lysate of the cell line UT-SCC-24A (WC 24A, Fig. 5B) when compared to UT-SCC-24B (WC 24B, Fig. 5B). The band intensity/densitometry value for E2F4 in the nucleus was only **7%** higher in UT-SCC-24B (N 24B, Fig. 5D) compared to UT-SCC-24A (N 24A, Fig. 5D). Furthermore, in Figure 5F, the intensity values of E2F4 in the cytoplasmic fraction was clearly higher in the cell line UT-SCC-24B (C 24B, Fig. 5F) compared to UT-SCC-24A (C 24A, Fig. 5F), showing about **39%** intensification.

Fold difference in expression of E2F4 in all of the cellular fractions (Whole cell (WC), nuclear (N) and cytoplasmic (C)) of the primary cell line UT-SCC-24A in comparison to the metastatic cell line UT-SCC-24B were calculated and are given in Figure 6. These results indicate that the levels of E2F4 in the nuclear fractions were not significantly different between the two cell lines, which is also reflected in levels of E2F4 in the whole cell (N+C=WC). In contrast, the cytoplasmic fraction results have shown much higher levels of E2F4 in UT-SCC-24B than UT-SCC-24A.

3.2 E2F4 GENE EXPRESSION LEVELS IN THE CELL LINES UT-SCC-24A AND UT-SCC-24B

Accordingly, RT-qPCR results (from 3 different passages) for the relative E2F4 expression in the cell lines, UT-SCC-24A and UT-SCC-24B were collected and calculated (Fig. 7). The results show that there is no significant difference in gene expression of E2F4 in UT-SCC-24A compared to UT-SCC-24B and vice versa, both showing an average quantity of **1.1** ± standard error of mean (SEM) in the bar chart below (Fig. 7).

3.3 MiRNA-363 Transfection Effects on the Cell Line UT-SCC-24B

We performed three trials of transient lipid-based transfection of the cell line UT-SCC-24A and UT-SCC-24B with miRNA-363. Trials of both cell lines were ran parallel and showed similar results. The cell lines were visualized under an inverted phase-contrast microscope at 24 h, 48 h and 72 h after transfection. We included Scramble and Mock controls, and images of these were recorded (Fig. 8). Cell count was carried out after 72 h of transfection (Fig. 8). This was done to examine the cell lines reactivity to the transfection in accordance to changes in number of cells and morphology.

The results (Fig. 8) show no change in morphology in the transfected UT-SCC-24A (Fig. 8A) compared to it negative control, scramble (Fig. 8B) and the non-transfected cells, Mock (Fig. 8C), respectively. A small change in morphology was observed in UT-SCC-24B compared to the respective controls, in which cells seemed to be smaller and longer/stretched after transfection with miRNA-363 (Fig. 8D - F). Moreover, the number of cells was shown to be influenced by the miRNA-363 transfection in the cell line UT-SCC-24B with about **43%** decrease in number of transfected cells (Fig. 8D) compared to the control scramble (Fig. 8E) and about **49%** decrease compared to the control Mock (Fig. 8F). The cell count for the transfected UT-SCC-24A revealed no prominent change in the number of cells compared to the controls (Fig. 8A - C). Due to lack of detectable impact by miRNA-363 on the primary cell line UT-SCC-24A by, where cell survival and growth were unchanged, further analysis for the transfected cell line investigation continued with the transfected UT-SCC-24B only.

3.4 MiRNA-363 Transfected UT-SCC-24B Cell line Shows Decrease in E2F4 Expression

E2F4 bands were detected using the LAS-4000 Imaging System at about 50-60 kDa (Fig. 9A, C and E). The E2F4 densitometry values were collected from the Image Studio Lite software, normalized to the corresponding loading control and are presented in the bar charts below (Fig. 9B, D and F).

Transfection with miRNA-363-5p showed reduced the band intensity values of E2F4 in the whole cell lysate to about **27%** compared to transfection with Scramble and to about **22%** compared to Mock transfection (Fig. 9B). In the nuclear fraction, an increase of **10%** was observed in E2F4 band intensity values in UT-SCC-24B cells transfected with miRNA-363-5p

compared to Scramble; and about **4%** increase when compared to Mock (Fig. 9D). Furthermore, the cytoplasmic fractions have shown a **41%** reduced intensification in E2F4 band intensity values of cells transfected with miRNA-363-5p compared to Scramble; and about **153%** decrease in comparison to Mock (Fig. 9F).

Fold difference was calculated for expression of E2F4 in all of the cellular fractions (WC, N and C) of the transfected metastatic cell line UT-SCC-24B compared to the transfection controls (Scramble and Mock) and are given in Figure 10. These results indicate that the levels of E2F4 in the nuclear fractions were not significantly different after 72 h transfection with miRNA-363. In contrast, the cytoplasmic fraction results have shown much lower levels of E2F4 in UT-SCC-24B after transfection, which is also reflected in levels of E2F4 in the whole cell (N+C=WC).

For verifications, two transfections of the cell line UT-SCC-24B were carried out, a replicate from the same passage and another passage. The results obtained from these analyses corresponded well for the WC fractions of transfected UT-SCC-24B, where a clear reduction in E2F4 levels was observed. However, blot quality for the N and C fractions did not qualify for comparable analysis (results not shown).

3.5 MiRNA-363 Target the Gene Expression of E2F4 in the Transfected UT-SCC-24B Cell line

Moreover, RT-qPCR results (from 5 different passages) for the relative E2F4 expression in the transfected UT-SCC-24B, along with the controls were collected and calculated (Fig. 11). The results show that E2F4 was downregulated in miRNA-363 transfected cell line displaying about **15%** reduction when compared the control Scramble. In contrast, **15%** increase in E2F4 expression was observed in the miRNA-363 transfected cell line in comparison to the control Mock (Fig. 11).

3.6 Histopathology of Oral Cancer Tissue

Immunohistochemistry analysis from three different OSCC patient , related to tongue, was conduct and the images of the slides were obtained by Olympus virtual slid scanner (Fig. 12). The results presented from patient I show an overview of the area of interest (Fig. 12A). Higher magnification from this image of relatively normal oral epithelium (OE) is presented in Figure

12B, showing little cytoplasmatic expression, and faint nuclear expression, mainly in the cells above the basal cell layer. Figure 12C show areas from the same section of malignant epithelial cells. Here, not only does the nucleus stain stronger, but also stronger cytoplasmatic expression can be observed.

Result from patient II are presented in similar panel setup. Figure 12E shows a magnified area of the overview (Fig. 12D), showing two areas of OE that display little cytoplasmic expression. In the OE of the lower left corner similar lack of nucleus staining in the basal cell layer can be observed (arrow). Interestingly, patches of epithelial tissue with malignant development display stronger coloration of the nuclei and cytoplasm here (asterisk), and especially in the deeper areas of invasive front, rich in tumor buds (Fig. 12F).

This pattern was even stronger displayed in patient III where the magnification on the overview (Fig. 12G) show little cytoplasmic coloration in the OE, and almost none in the basal cell layer of it (Fig. 12H). Also here, deeper and well differentiated more malignant epithelial cells stained stronger in general, and in their cytoplasm.

3.7 RESULTS FIGURES AND LEGENDS

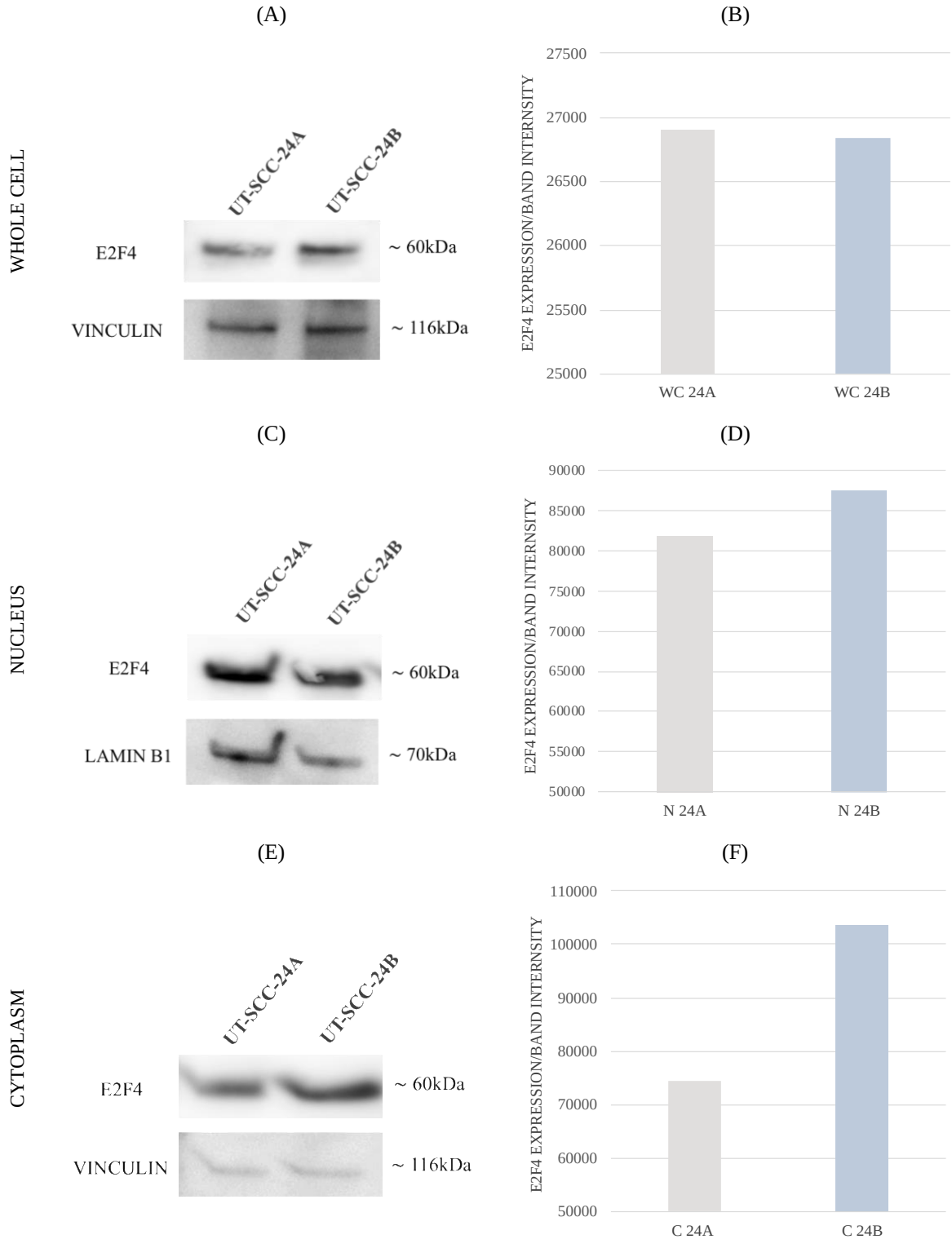

Figure 5: Western blot and its densitometric analysis for the whole cell (WC), nuclear (N) and cytoplasmic (C) fractions of the cell lines UT-SCC-24A and 24B. *Loaded samples (A, C, E) were treated with Anti-E2F4 rabbit primary Antibody (1:5000) followed by detection with anti-rabbit secondary antibody (1:1000). The WC and C membranes were probed with Vinculin antibody (1:400), while the N membranes with Lamin B1 antibody (1:5000). Bar charts (B, D and F) showing the levels of*

E2F4 of the different cellular fractions of UT-SCC-24A compared to UT-SCC-24B. Detection and data quantification and normalization was done as mentioned in the methods.

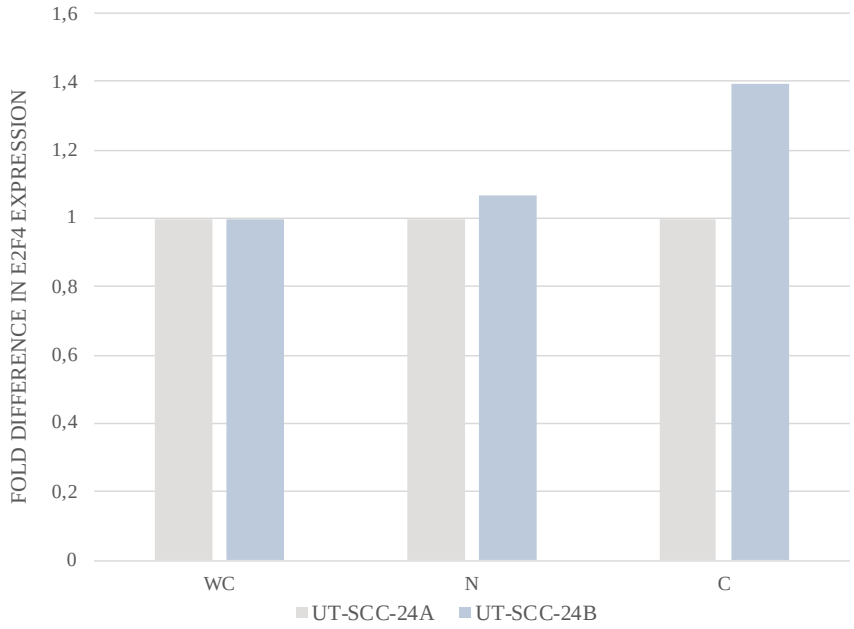

Figure 6: Fold difference in the levels of E2F4 in the whole cell (WC), nuclear (N) and cytoplasmic (C) fractions of the cell lines UT-SCC-24A and 24B. *The fold changes in E2F4 observed for WC and N fractions were not significant. Cytoplasmic fractions however showed elevated E2F4 levels in UT-SCC-24B compared to UT-SCC-24A. Densitometric analysis values of the western blots in figure-1 were used to calculate the fold difference in E2F4 levels in the different cellular fractions of UT-SCC-24A relative to UT-SCC-24B. Values were normalized to the corresponding loading control.*

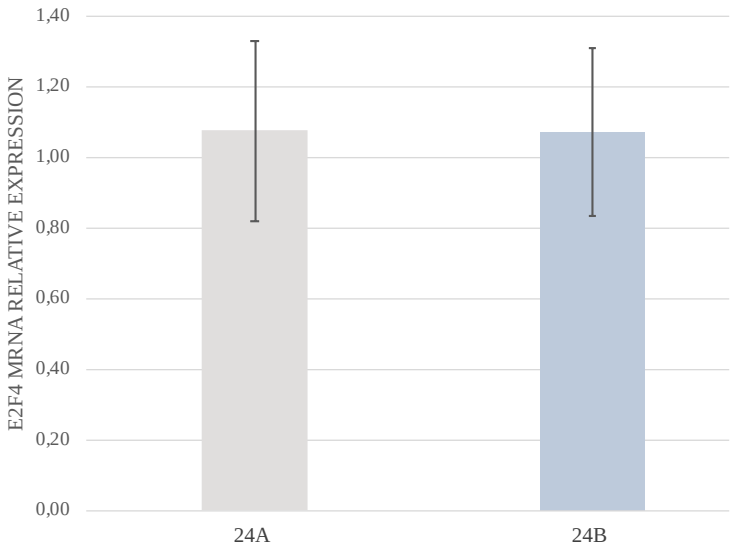

Figure 7: RT-qPCR analysis for the relative expression of E2F4 in the cell lines UT-SCC-24A and UT-SCC-24B. *The cell lines were cultured in 10% FBS DMEM and harvested at 80-90% confluency. Harvested cells were isolated for RNA and run for RT-qPCR analysis, using the SybrGreen dye assay, in a LightCycler 96 machine. Homo Sapiens β-actin, eF1a and B2M were used as the reference genes. The qPCR data of three trials were calculated and represented as a mean ± standard error of mean (SEM).*

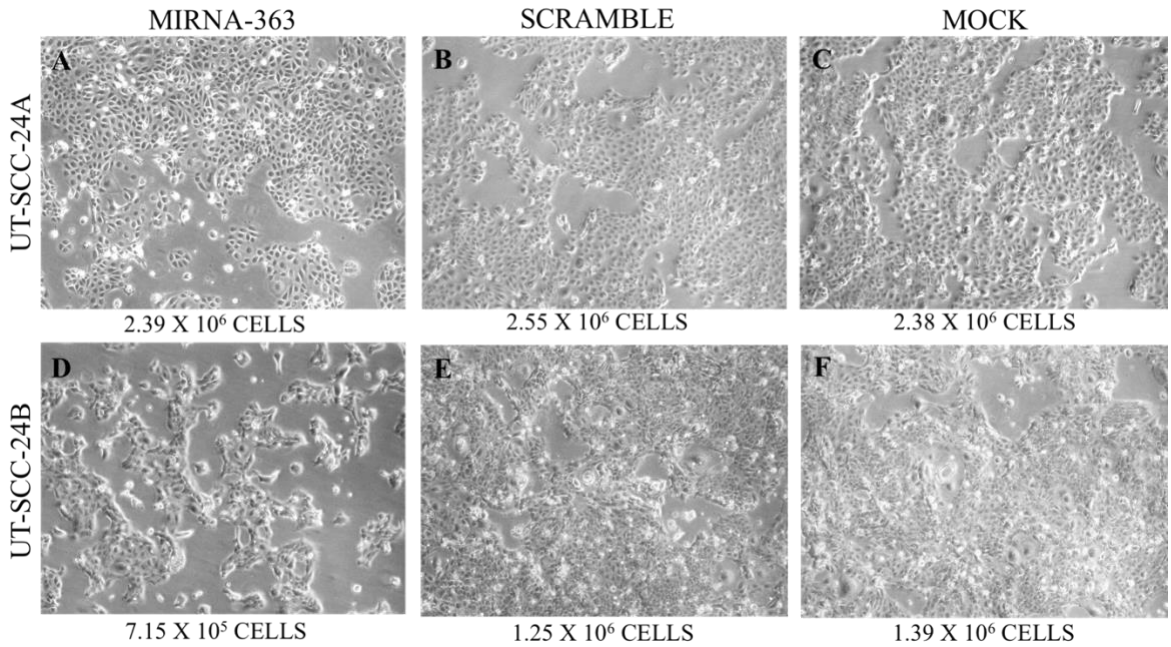

Figure 8: Inverted phase-contrast microscopy images of the cell line UT-SCC-24A and UT-SCC-24B after 72 h transfection with miRNA-363, including the control Scramble and Mock. *Adherent cell lines (A - F) show an epithelial-like morphology with polygonally shaped cells, with slightly more elongated/stretched-like and irregular shaped UT-SCC-24B cells (D - F) compared to UT-SCC-24A cells (A – C). All images were taken with a digital camera at 100x magnification. All images display completely intact layer of confluent growth of the cell lines.*

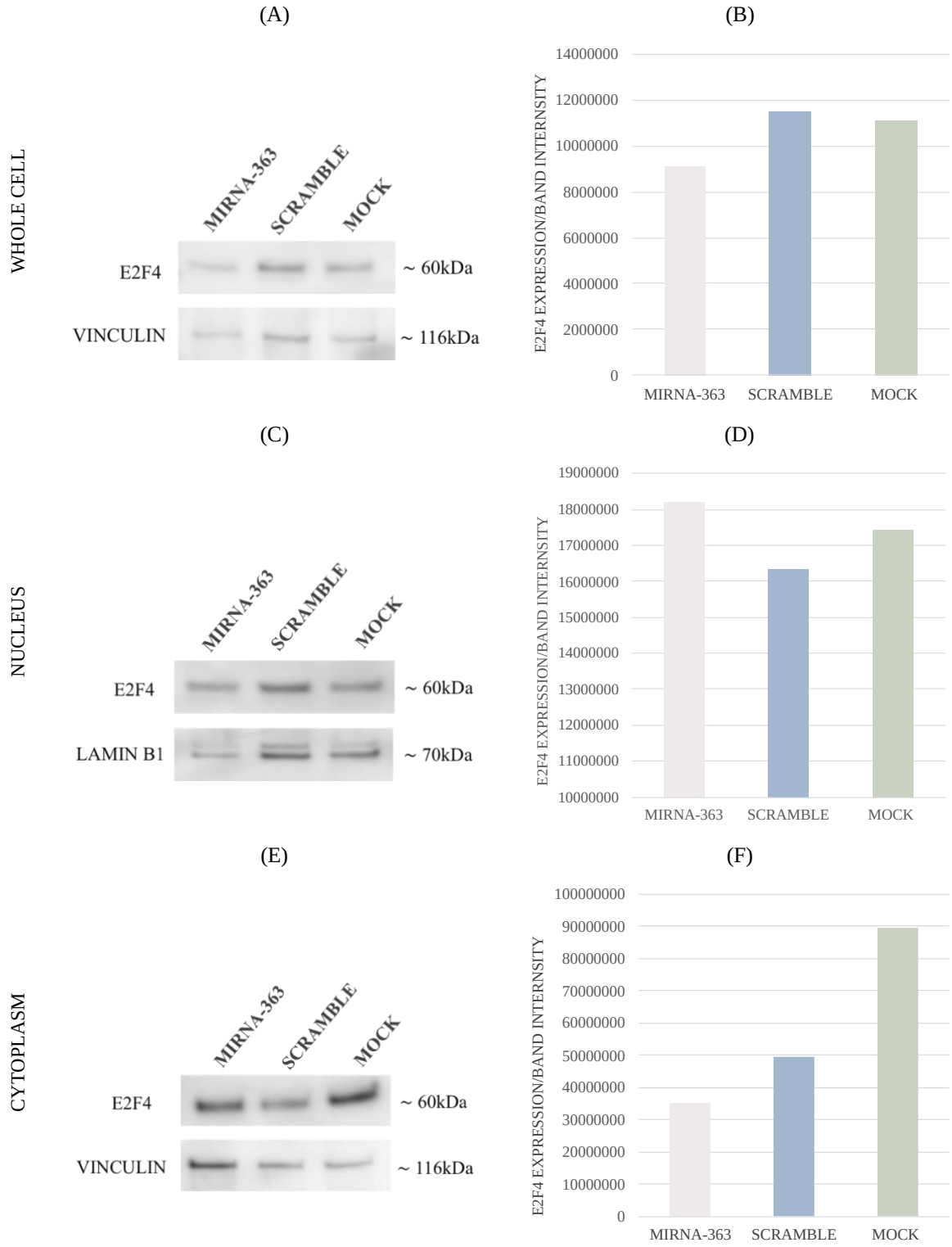

Figure 9: Western blot and its densitometric analysis of whole cell (WC), nuclear (N) and cytoplasmic (C) fractions of the transfected cell line UT-SCC-24B. *The cell line UT-SCC-24B was transfected with miRNA-363-5p (miRNA), Scramble and Mock as controls for 72 h. Loaded samples (A, C and E) were treated with Anti-E2F4 rabbit primary Antibody (1:5000) followed by detection with anti-rabbit secondary antibody (1:1000). Vinculin (1:400) and Lamin B1 (1:5000) were used as the loading controls. Detection was performed as mentioned in the methods. Bar charts (B, D and F) showing the levels of E2F4 of the different cellular fractions of the miRNA-363 transfected UT-SCC-24B in comparison to the controls respectively. Data quantification and normalization was done as mentioned in the methods.*

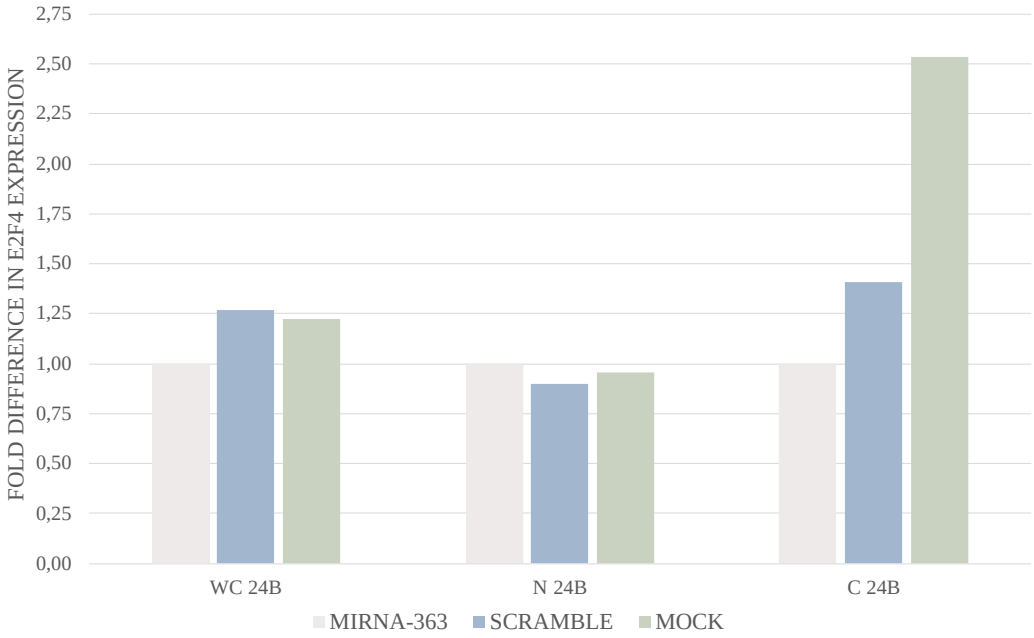

Figure 10: Fold difference in the levels of E2F4 for the cell line UT-SCC-24B in different cellular compartments, whole cell (WC), nuclear (N) and cytoplasmic (C), after 72 h transfection with miRNA-363 compared to the controls (Scramble and Mock). *The fold changes in E2F4 observed for the N fractions were not significant. The WC and C fractions however showed a clear diminished E2F4 levels in UT-SCC-24B after transfection with miRNA-363 in comparison the controls. Densitometric analysis values of the western blots in figure-4 were used to calculate the fold difference in E2F4 levels in the different cellular fractions of transfected UT-SCC-24B relative to Scramble and Mock. Values were normalized to the corresponding loading control.*

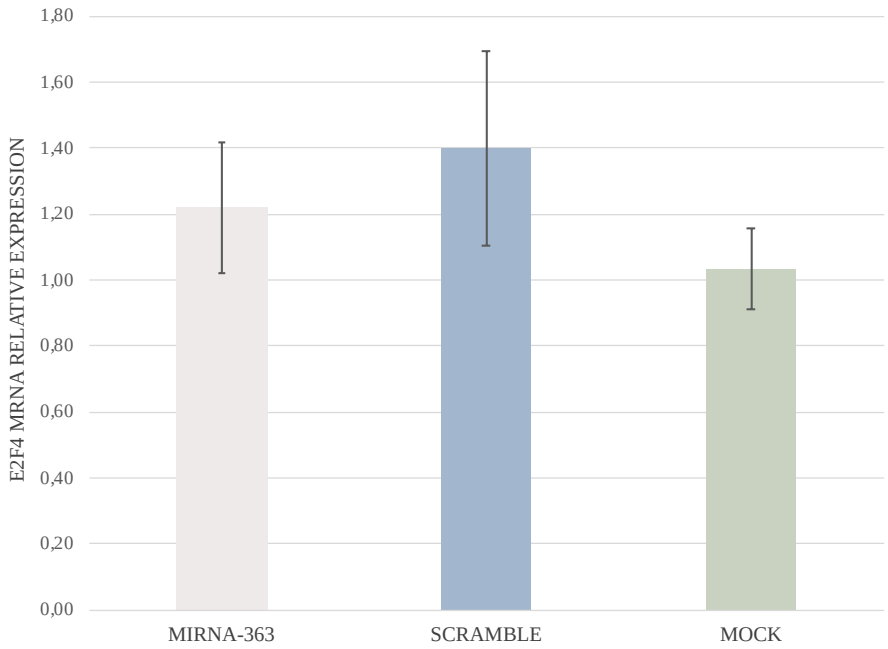

Figure 11: RT-qPCR analysis for the relative expression of E2F4 in the cell line UT-SCC-24B. *The cell line was transiently transfected with miRNA-363, Scramble and Mock (as controls) for 72 h. Harvested cells were isolated for RNA and run for RT-qPCR analysis, using the SybrGreen dye assay, in a LightCycler 96 machine. Homo Sapiens β-actin, eF1a and B2M were used as the reference genes. The qPCR data of five trials were calculated and represented as a mean ± standard error of mean (SEM).*

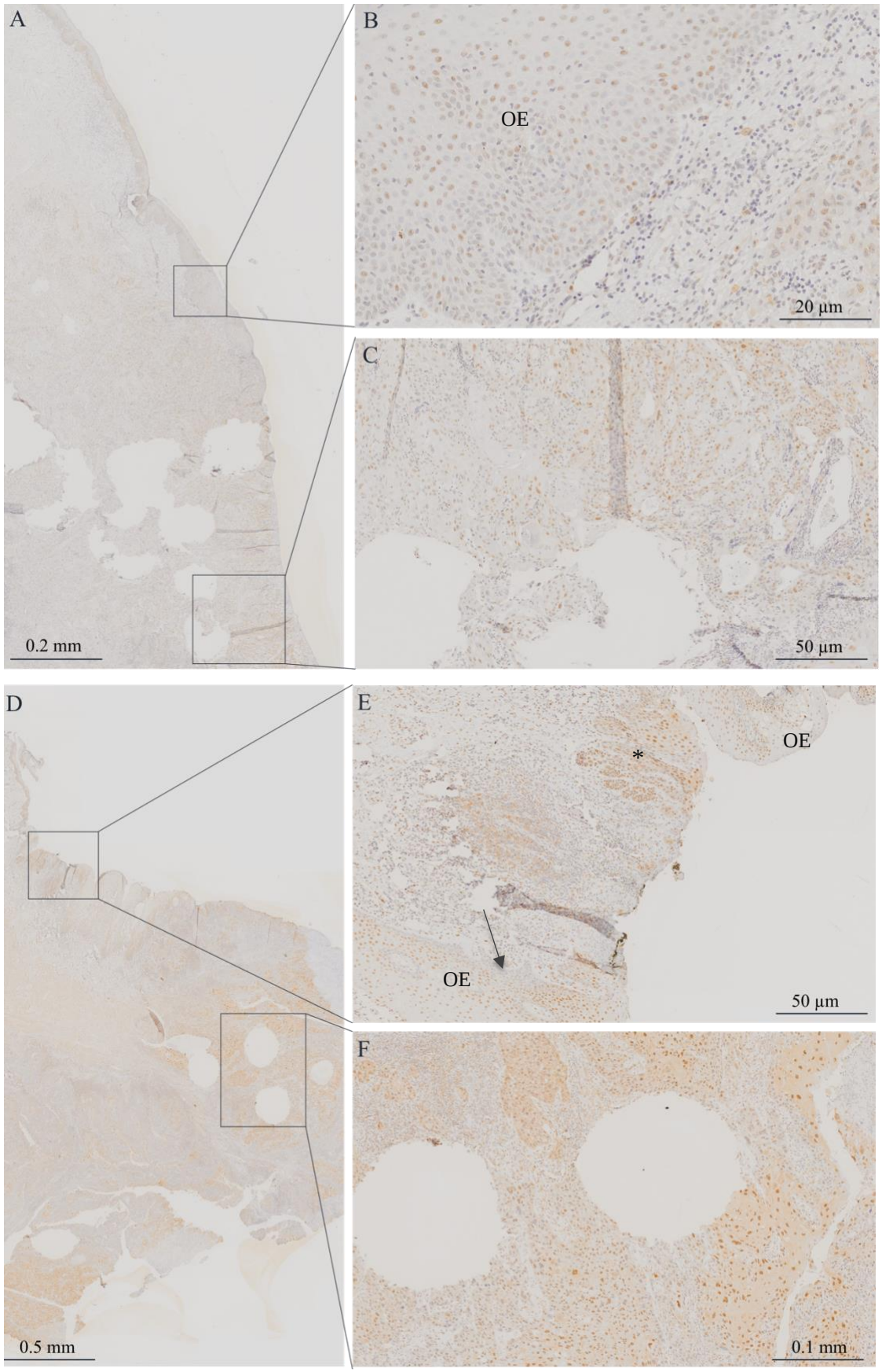
PATIENT I
PATIENT II
A
B
OE
20 µm
C
0.2 mm
50 µm
D
E
*
OE
OE
50 µm
F
0.5 mm
0.1 mm

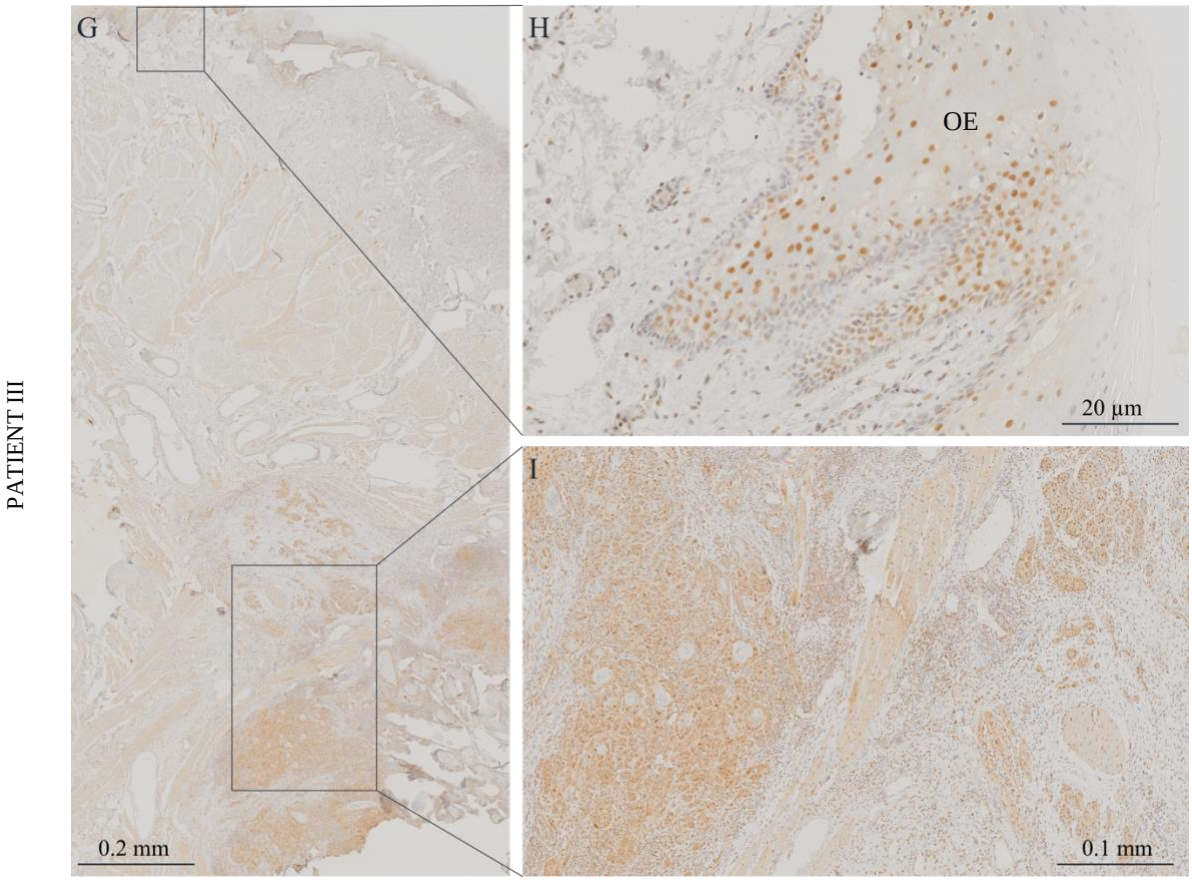

Figure 12: Detection of E2F4 in human tongue tissue from three oral cancer patients (I-III) by IHC. *IHC staining for E2F4 in a formalin fixed paraffin embedded (FFPE) section of human tongue tissue was done using a rabbit monoclonal anti-E2F4 antibody as the primary antibody and an anti-rabbit IgG-HRP conjugate as the secondary antibody as described in the method. (A, D and G) represent an overview of the stained tissue at 1.1X, 0.74X and 0.9X magnifications, respectively. At different magnifications, B(11.23X), E(4.24X), and H(10.57X) represent shallower area/regions closer to the edges, showing lower tumor budding where E2F4 expression is minimal and only present in the nucleus of the cell. (C, F and I) represent deeper areas in the tissues (taken at 4.24X, 3.27X and 3.4X) showing higher tumor budding where E2F4 is all over the cell inside nucleus and the cytoplasm. OE: Oral Epithelium.*

4 DISCUSSION

One of the major hallmarks of carcinogenesis is the dysregulation of cell cycle machinery, which involves all of the signaling pathways linked to the cell cycle control system. Hence cell cycle regulators and control persist to be a predominant theme of human carcinogenesis which is also known to occur in OSCC (2, 4, 5, 41). Therefore, it's important to understand how these pathways are stimulated and/or inhibited during tumorigenesis.

The purpose of this study was to investigate an interesting but little studied cell cycle related protein, E2F4, in oral cancer cells and tissues, as well as to evaluate it for any clinical value perhaps in combination with miRNA-363. Using miRNA transfection, Western blot and RT-qPCR of the oral cancer cell lines, along with immunohistochemistry analysis of oral cancer tissues, we were able to demonstrate that both miRNA-363 and E2F4 may be enriching for our understanding, and hence for the treatment, of OSCC.

4.1 THE SIGNIFICANCE OF SUB-CELLULAR LOCALIZATION OF E2F4

Our WB results showed a stronger cytoplasmic expression of E2F4 in the cancer cell line with higher association to metastasis (UT-SCC-24B) when compared to the cell line with lower association to metastasis (UT-SCC-24A), leading us to hypothesize that malignancy was linked to cytoplasmic expression of the protein. The hypothesis gained further support in our IHC-study of tissues from three different OSCC patients. Here E2F4 was found highly expressed, both in the nucleus and the cytoplasm of the well differentiated and more malignant areas of the tumor; i.e. at the invasive front and in tumor buds. The observation which further complemented our assumption is when the nearby parts of more normal oral epithelium mainly displayed coloration in the nucleus. Furthermore, little or no staining was observed in the basal cell layer of the epithelium. This is an interesting finding. Although E2F4 is reported to be constitutively expressed throughout the cell cycle and is understood to be a vital regulator of the cell cycle with two main functions: cell cycle arrest and cell proliferation (which is broadly involved in carcinogenesis and the severity of cancer), (52, 55, 86, 87) very few have linked it to cell motility regulation and the tumor metastatic process (88), as our results of the basal cell layers may support.

To further verify these findings, we separated the nucleus from cytoplasm in our cells lines and compared them. Both nuclear and cytoplasmic fractions of UT-SCC-24B showed higher

amount of protein. However, the fold-change difference clearly displayed a stronger increase in the cytoplasmic fraction.

Previous studies show E2F4's nuclear localization to be important during the G0 and early G1 phase of the cell cycle in association with the Rb protein family. Furthermore, E2F4 experiences a gradual increase in cytoplasmic localization as the cell proceed toward the S phase, i.e. during dividing/proliferating/cycling cells (42, 54, 56, 89). These results also indicate that overexpression in the cytoplasm correlates with increased invasiveness and metastasis, which have also been reported, where patients showing high expression of E2F4 target genes exhibit more severe cancer and shorter survival (86, 87, 90, 91). However, very few have been linked to OSCC. E2F4 levels have been reported to be elevated in more advanced and metastatic breast cancer patients (42, 45, 92), prostate cancer patients (42) and in Acute Myeloid Leukaemia (93).

Such pattern subcellular location and its importance to cancer have been found in other studies as well, p27 is also found to be aberrantly located in the cytoplasm in many cancers including breast, thyroid, esophageal colorectal, and nasopharyngeal carcinomas, and sarcoma (94-97). It was also observed to correlate with poor survival in breast cancer and nasopharyngeal carcinoma patients when seen in the cytoplasm (N+C) rather than in the nucleus alone (N) (95, 96). Along with p27, a wide of range of tumor suppressors including Rb, p53, and cell cycle regulators, such as p21, and E2F4 have been reported to only be protective against tumorigenesis when residing in the nucleus and to be abnormally delocalized in most cancers (94, 97). Although many of these findings are not directly linked to E2F4, these studies do add confidence to the work presented here.

4.2 E2F4 Gene expression Trends

E2F4 relative mRNA expression was also studied via RT-qPCR of the oral cancer cell lines UT-SCC-24A and 24B, where no significant change in mRNA expression was observed. This indicate that regulatory activity of E2F4 cannot be reflected by mRNA level probably due to post-transcriptional and post-translational control mechanisms, which has been previously reported (58, 98).

4.3 E2F4 Regulation by MiRNA-363 in the Oral Cancer Cell Lines

Using the web server, TargetScan, we predicted possible regulatory interplay between miRNA-363-5p and E2F4. Although a number of miRNAs have been reported to be involved in HNSCCs and OSCCs (5, 22, 25, 29, 30), cancers with low miRNA-363 expression level and high E2F4 levels, have been reported to be involved with poor prognosis (99). However, very little has been reported about the relationship between them in OSCC.

To test the potential regulatory effects of miRNA-363 on the expression of the transcription factor E2F4, transient transfection of oral cancer cell lines, UT-SCC-24A and UT-SCC-24B was carried out. Our results here suggest morphological changes and demonstrated nearly 50% cell death in UT-SCC-24B cell line after transfection with miRNA-363-5p. These changes were not observed in the less metastatic cell line, UTSCC-24-A.

Confirming this, Western blot of the transfected UT-SCC-24B cells, showed E2F4 expression to be reduced by about 25%. For verifications, two additional WB-trials of the transfected cell line UT-SCC-24B were carried out, one being a replicate. The results obtained here corresponded well and verified our presented data (Fig. 9B). These findings support the results of the greatly reduced cell survival and growth observed in the metastatic cell line UT-SCC-24B upon transfection with miRN-363.

Furthermore, we attended to demonstrated changes in the cytoplasmic (C) and nuclear (N) fractions of the transfected UT-SCC-24B cells. A clear reduction was observed in C fraction and a minor increase, of about 7%, was observed in the N fraction. This is in comparison to C and N respective Scramble and Mock controls. However, the verification trials here failed to provide the necessary inter-comparable analysis and hence have not been further verified.

Overall, the findings related to miRNA-363 here, are also interesting as they are in line with the preliminary findings (not published) from a major ongoing project regarding OSCC, namely NOROC (Norwegian Oral cancer Study, led by Tumor Biology Research Group (Department of Medical Biology, The Faculty of Health Sciences, University of Tromsø, The Arctic University of Norway, Norway). Here, the preliminary NGS-data of oral cancer tissue from 89 patients show low or no expression of the hsa-miR-363-5p. Although these data are still to be statistically managed and verified, they add support to our hypothesis and are highly suggestive of OSCC's need to keep its expressions levels of miRNA-363-5p low, in order to advance its

malignancy. Other studies have also reported low or downregulated expression of miRNA-363 in number of human cancers, including head and neck cancers, and its correlation with poor prognosis (28, 100).

Also, RT-qPCR of the miRNA-363 transfected UT-SCC-24B, found mRNA expression of E2F4 downregulated by about 15% compared to the control Scramble, which was in line with the Western blot results. miRNA can regulate the gene expression both at the level of transcription and translation. However, there are several reports of miRNA targets for which translational repression is detected without observable changes in the mRNA level, indicating that miRNA control may occur independently of mRNA decay for these targets, corresponding to what we have elucidated here (101, 102).

4.4 Future Perspectives

Despite the shortcomings, there is sufficient evidence to suggest that E2F4 have a molecular relationship to OSCCs, in which its expression pattern may strongly correlates with increased invasiveness and metastases and ultimately poor prognosis. This would be in line with similar findings which have validated the molecular relevance and prognostic value of E2F4 in other cancers including HNSCCs.

Hence, further research should aim at conducting more replications and establishing better methods to study the nuclear and cytoplasmic fractions for more significant results. Along with replication and verification studies, evaluation for better controls should be ongoing. Controls for IHC in this study were limited for our specific antibody, hence better controls and perhaps an additional E2F4-antibody should be aimed at in future study.

Immunofluorescence analysis of the cell lines should be included, as it may serve better as a qualitative and semi-quantitative method compared to WB and RT-qPCR. Further studies of other malignant cell lines related to OSCC, treated with mir363, should be carried out to verify similar outcome, especially concerning its potency for inflicting cell death.

Regarding IHC-analysis, this study evaluated only three patients for IHC-analysis, and all three displayed the same pattern, confirming our main hypothesis. This 100% positive outcome may be misleading, and hence a bigger selection of whole tissue sections is needed to confirm the reliability. Furthermore, in situ hybridization (ISH) of miRNA of the same sections should be

carried out, to evaluate not only the possible biomarker role of it, but to determine complementary staining pattern with E2F4. This may help in creating an even more reliable "biomarker sets". Related to this, it may be interesting to also study E2F5 (42, 55), as it is often seemed to play similar role as E2F4 as well other cell cycle regulators proteins like p27, as it showed similar subcellular expression patterns as E2F4, which will aid in creating biomarkers sets.

Also, IHC of tissue micro array (TMA) have already been tested, with interesting outcomes of the corresponding survival data (not shown). However, it is our current understanding that scoring of these depends on where the cores have been selected from in the tissue block. Given the dynamic and selective staining pattern of E2F4, the TMA results may therefore be somewhat misleading. However, if the TMAs are selected and marked selectively for early dysplasia/normal epithelium Vs invasive front/tumor buds, the method may prove time worthy, especially given that E2F4 could hold prognostic value and perhaps even serve as a novel treatment in combination with miRNA-363 in OSCCs.

5 CONCLUSION

In conclusion, our findings show E2F4 to be highly expressed in the cytoplasm of the cell line UT-SCC-24B. Also, miRNA-363 have demonstrated regulatory outcomes on E2F4 in the transfected UT-SCC-24B cell line. These results are very promising and despite that some of data presented here are somewhat lacking in their detail, it is clear that E2F4 and miRNA-363 and the pathways they may be involved in, deserve a better understanding, especially in OSCC. Furthermore, due to the findings of E2F4's dynamic expression pattern, this study also proposes E2F4 as a potential biomarker for OSCC, as well as contribute to our understanding of its tumor biology. However, our knowledge is still limited, when it comes to E2F4 and miRNA-363 association in OSCC. Future studies should therefore not only recur these findings, but also focus on the biological mechanisms and timeframe that may further clarify the elusive subcellular location of E2F4.

BIBLIOGRAPHY

1. Alberts B, Johnson A, Lewis J, Morgan D, Raff M, Roberts K, et al. Molecular Biology of the Cell, Sixth Edition: Garland Science, Taylor & Francis Group; 2015.

2. Weinberg RA. The biology of cancer. 2nd ed. ed. New York: Garland Science; 2014.

3. Khurshid Z, Zafar MS, Khan RS, Najeeb S, Slowey PD, Rehman IU. Chapter Two - Role of Salivary Biomarkers in Oral Cancer Detection. In: Makowski GS, editor. Advances in Clinical Chemistry. 86: Elsevier; 2018. p. 23-70.

4. Rivera C. Essentials of oral cancer. International journal of clinical and experimental pathology. 2015;8(9):11884-94.

5. Leemans CR, Braakhuis BJM, Brakenhoff RH. The molecular biology of head and neck cancer. Nature Reviews Cancer. 2010;11:9.

6. Cristaldi M, Mauceri R, Di Fede O, Giuliana G, Campisi G, Panzarella V. Salivary Biomarkers for Oral Squamous Cell Carcinoma Diagnosis and Follow-Up: Current Status and Perspectives. Front Physiol. 2019;10:1476-.

7. Solomon B, Young RJ, Rischin D. Head and neck squamous cell carcinoma: Genomics and emerging biomarkers for immunomodulatory cancer treatments. Seminars in cancer biology. 2018;52(Pt 2):228-40.

8. O'Neill JP, Shah JP. Self-Assessment in Head and Neck Surgery and Oncology E-Book: Elsevier Health Sciences; 2014.

9. Sasahira T, Kirita T. Hallmarks of Cancer-Related Newly Prognostic Factors of Oral Squamous Cell Carcinoma. Int J Mol Sci. 2018;19(8):2413.

10. Jiang S, Dong Y. Human papillomavirus and oral squamous cell carcinoma: A review of HPV-positive oral squamous cell carcinoma and possible strategies for future. Current Problems in Cancer. 2017;41(5):323-7.

11. WHO. Cancer - Oral cancer: WHO; 2020 [Available from: https://www.who.int/cancer/prevention/diagnosis-screening/oral-cancer/en/.

12. Liu L, Chen J, Cai X, Yao Z, Huang J. Progress in targeted therapeutic drugs for oral squamous cell carcinoma. Surgical Oncology. 2019;31:90-7.

13. Ghantous Y, Yaffi V, Abu-Elnaaj I. [Oral cavity cancer: epidemiology and early diagnosis]. Refu'at ha-peh veha-shinayim (1993). 2015;32(3):55-63, 71.

14. Marur S, Forastiere AA. Head and Neck Squamous Cell Carcinoma: Update on Epidemiology, Diagnosis, and Treatment. Mayo Clinic proceedings. 2016;91(3):386-96.

15. Rapado-González O, Martínez-Reglero C, Salgado-Barreira A, López-López R, Suárez-Cunqueiro MM, Muinelo-Romay L. miRNAs in liquid biopsy for oral squamous cell carcinoma diagnosis: Systematic review and meta-analysis. Oral oncology. 2019;99:104465.

16. Mishra R. Cell cycle-regulatory cyclins and their deregulation in oral cancer. Oral oncology. 2013;49(6):475-81.

17. Shang A, Lu W-Y, Yang M, Zhou C, Zhang H, Cai Z-X, et al. miR-9 induces cell arrest and apoptosis of oral squamous cell carcinoma via CDK 4/6 pathway. Artificial Cells, Nanomedicine, and Biotechnology. 2018;46(8):1754-62.

18. Esteller M. Non-coding RNAs in human disease. Nature Reviews Genetics. 2011;12(12):861-74.

19. Hammond SM. An overview of microRNAs. Adv Drug Deliv Rev. 2015;87:3-14.

20. O'Brien J, Hayder H, Zayed Y, Peng C. Overview of MicroRNA Biogenesis, Mechanisms of Actions, and Circulation. Frontiers in Endocrinology. 2018;9(402).

21. Macfarlane L-A, Murphy PR. MicroRNA: Biogenesis, Function and Role in Cancer. Curr Genomics. 2010;11(7):537-61.

22. Hayes J, Peruzzi PP, Lawler S. MicroRNAs in cancer: biomarkers, functions and therapy. Trends in molecular medicine. 2014;20(8):460-9.

23. Zhang C. Novel functions for small RNA molecules. Curr Opin Mol Ther. 2009;11(6):641-51.

24. Liu H, Lei C, He Q, Pan Z, Xiao D, Tao Y. Nuclear functions of mammalian MicroRNAs in gene regulation, immunity and cancer. Molecular Cancer. 2018;17(1):64.

25. Huang W. MicroRNAs: Biomarkers, Diagnostics, and Therapeutics. Methods in molecular biology (Clifton, NJ). 2017;1617:57-67.

26. Liu B, Shyr Y, Cai J, Liu Q. Interplay between miRNAs and host genes and their role in cancer. Briefings in Functional Genomics. 2019;18(4):255-66.

27. Ha M, Kim VN. Regulation of microRNA biogenesis. Nature reviews Molecular cell biology. 2014;15(8):509-24.

28. Sun Q, Zhang J, Cao W, Wang X, Xu Q, Yan M, et al. Dysregulated miR-363 affects head and neck cancer invasion and metastasis by targeting podoplanin. The International Journal of Biochemistry & Cell Biology. 2013;45(3):513-20.

29. Fukumoto I, Hanazawa T, Kinoshita T, Kikkawa N, Koshizuka K, Goto Y, et al. MicroRNA expression signature of oral squamous cell carcinoma: functional role of microRNA-26a/b in the modulation of novel cancer pathways. British journal of cancer. 2015;112(5):891-900.

30. Ghffari M, Asadi M, Shanaehbandi D, Bornehdeli S, Sadeghzadeh M, Mohammad Reza Khani H, et al. Aberrant Expression of miR-103, miR-184, miR-378, miR-497 and miR-506 in Tumor Tissue from Patients with Oral Squamous Cell Carcinoma Regulates the Clinical Picture of the Patients. Asian Pacific journal of cancer prevention : APJCP. 2020;21(5):1311-5.

31. Ross JP, Kassir Z. The varied roles of nuclear argonaute-small RNA complexes and avenues for therapy. Mol Ther Nucleic Acids. 2014;3(10):e203-e.

32. Bueno MJ, Malumbres M. MicroRNAs and the cell cycle. Biochimica et Biophysica Acta (BBA) - Molecular Basis of Disease. 2011;1812(5):592-601.

33. Cofre J, Abdelhay E. Cancer Is to Embryology as Mutation Is to Genetics: Hypothesis of the Cancer as Embryological Phenomenon. The Scientific World Journal. 2017;2017:17.

34. Ma Y, Zhang P, Wang F, Yang J, Yang Z, Qin H. The relationship between early embryo development and tumourigenesis. Journal of cellular and molecular medicine. 2010;14(12):2697-701.

35. Sonnenschein C, Soto AM. Carcinogenesis explained within the context of a theory of organisms. Progress in biophysics and molecular biology. 2016;122(1):70-6.

36. WHO. Cancer: WHO; [updated 12.09.2018. Available from: https://www.who.int/news-room/fact-sheets/detail/cancer.

37. Orloff DG. Cancer Development: CancerQuest; [Available from: https://www.cancerquest.org/cancer-biology/cancer-development.

38. Lakshminarayana S, Augustine D, Rao RS, Patil S, Awan KH, Venkatesiah SS, et al. Molecular pathways of oral cancer that predict prognosis and survival: A systematic review. Journal of carcinogenesis. 2018;17:7.

39. Kotecha R, Takami A, Espinoza JL. Dietary phytochemicals and cancer chemoprevention: a review of the clinical evidence. Oncotarget. 2016;7(32):52517-29.

40. Cooper GM. The cell : a molecular approach. Washington, D.C. :Sunderland, Mass.: ASM Press; Sinauer Associates; 2000.

41. Hanahan D, Weinberg Robert A. Hallmarks of Cancer: The Next Generation. Cell. 2011;144(5):646-74.

42. Hsu J, Sage J. Novel functions for the transcription factor E2F4 in development and disease. Cell Cycle. 2016;15(23):3183-90.

43. Leal-Esteban LC, Fajas L. Cell cycle regulators in cancer cell metabolism. Biochimica et Biophysica Acta (BBA) - Molecular Basis of Disease. 2020;1866(5):165715.

44. Weijts BGMW, Bakker WJ, Cornelissen PWA, Liang K-H, Schaftenaar FH, Westendorp B, et al. E2F7 and E2F8 promote angiogenesis through transcriptional activation of VEGFA in cooperation with HIF1. The EMBO Journal. 2012;31(19):3871-84.

45. Schaal C, Pillai S, Chellappan SP. Chapter Four - The Rb–E2F Transcriptional Regulatory Pathway in Tumor Angiogenesis and Metastasis. In: Tew KD, Fisher PB, editors. Advances in Cancer Research. 121: Academic Press; 2014. p. 147-82.

46. Visconti R, Della Monica R, Grieco D. Cell cycle checkpoint in cancer: a therapeutically targetable double-edged sword. Journal of Experimental & Clinical Cancer Research. 2016;35(1):153.

47. Reece JB, Campbell NA. Campbell biology. Boston: Benjamin Cummings / Pearson; 2011.

48. Mens MMJ, Ghanbari M. Cell Cycle Regulation of Stem Cells by MicroRNAs. Stem Cell Rev Rep. 2018;14(3):309-22.

49. Kwak PB, Iwasaki S, Tomari Y. The microRNA pathway and cancer. Cancer Science. 2010;101(11):2309-15.

50. Cuitiño MC, Pécot T, Sun D, Kladney R, Okano-Uchida T, Shinde N, et al. Two Distinct E2F Transcriptional Modules Drive Cell Cycles and Differentiation. Cell Rep. 2019;27(12):3547-60.e5.

51. Ouseph Madhu M, Li J, Chen H-Z, Pécot T, Wenzel P, Thompson John C, et al. Atypical E2F Repressors and Activators Coordinate Placental Development. Developmental Cell. 2012;22(4):849-62.

52. Attwooll C, Denchi EL, Helin K. The E2F family: specific functions and overlapping interests. The EMBO Journal. 2004;23(24):4709-16.

53. Pundir S, Martin MJ, O'Donovan C. UniProt Protein Knowledgebase. In: Wu CH, Arighi CN, Ross KE, editors. Protein Bioinformatics: From Protein Modifications and Networks to Proteomics. New York, NY: Springer New York; 2017. p. 41-55.

54. Trimarchi JM, Lees JA. Sibling rivalry in the E2F family. Nature Reviews Molecular Cell Biology. 2002;3:11.

55. Kent LN, Leone G. The broken cycle: E2F dysfunction in cancer. Nature Reviews Cancer. 2019;19(6):326-38.

56. Russo G, Zamparelli A, Howard CM, Minimo C, Bellan C, Carillo G, et al. Expression of Cell Cycle–Regulated Proteins pRB2/p130, p107, E2F4, p27, and pCNA in Salivary Gland Tumors: Prognostic and Diagnostic Implications. Clinical Cancer Research. 2005;11(9):3265-73.

57. Deschênes C, Alvarez L, Lizotte ME, Vézina A, Rivard N. The nucleocytoplasmic shuttling of E2F4 is involved in the regulation of human intestinal epithelial cell proliferation and differentiation. Journal of cellular physiology. 2004;199(2):262-73.

58. Li Y, Huang J, Yang D, Xiang S, Sun J, Li H, et al. Expression patterns of E2F transcription factors and their potential prognostic roles in breast cancer. Oncol Lett. 2018;15(6):9216-30.

59. Torre Lindsey A, Bray F, Siegel Rebecca L, Ferlay J, Lortet‐Tieulent J, Jemal A. Global cancer statistics, 2012. CA: A Cancer Journal for Clinicians. 2015;65(2):87-108.

60. Oliveira LR, Ribeiro-Silva A. Prognostic significance of immunohistochemical biomarkers in oral squamous cell carcinoma. International journal of oral and maxillofacial surgery. 2011;40(3):298-307.

61. Philippeos C, Hughes RD, Dhawan A, Mitry RR. Introduction to cell culture. Methods in molecular biology (Clifton, NJ). 2012;806:1-13.

62. Bairoch A. The Cellosaurus: a cell line knowledge resource [updated 28.05.2018. Available from: https://web.expasy.org/cellosaurus/.

63. Huang H-L, Hsing H-W, Lai T-C, Chen Y-W, Lee T-R, Chan H-T, et al. Trypsin-induced proteome alteration during cell subculture in mammalian cells. J Biomed Sci. 2010;17(1):36-.

64. Blanco I. Chapter 3 - Alpha-1 Antitrypsin Biology. In: Blanco I, editor. Blanco's Overview of Alpha-1 Antitrypsin Deficiency: Academic Press; 2017. p. 23-37.

65. Rauch C, Feifel E, Amann EM, Spotl HP, Schennach H, Pfaller W, et al. Alternatives to the use of fetal bovine serum: human platelet lysates as a serum substitute in cell culture media. Altex. 2011;28(4):305-16.

66. Pegg DE. Principles of cryopreservation. Methods in molecular biology (Clifton, NJ). 2007;368:39-57.

67. Magi B, Liberatori S. Immunoblotting Techniques. In: Burns R, editor. Immunochemical Protocols. Totowa, NJ: Humana Press; 2005. p. 227-53.

68. Mahmood T, Yang P-C. Western blot: technique, theory, and trouble shooting. N Am J Med Sci. 2012;4(9):429-34.

69. Pehkonen H, von Nandelstadh P, Karhemo P-R, Lepikhova T, Grenman R, Lehti K, et al. Liprin-α1 is a regulator of vimentin intermediate filament network in the cancer cell adhesion machinery. Scientific Reports. 2016;6(1):24486.

70. Johnson M, Labome. Loading Controls for Western Blots. Materials and Methods. 2012.

71. Gavini K, Parameshwaran K. Western Blot (Protein Immunoblot). StatPearls [Internet]: StatPearls Publishing; 2019.

72. Kim TK, Eberwine JH. Mammalian cell transfection: the present and the future. Anal Bioanal Chem. 2010;397(8):3173-8.

73. Livak KJ, Schmittgen TD. Analysis of Relative Gene Expression Data Using Real-Time Quantitative PCR and the 2−ΔΔCT Method. Methods. 2001;25(4):402-8.

74. Gabriela G, Julia B, Dijana D, Per‐Henrik E, Vikas M, M BB, et al. A systematic analysis of commonly used antibodies in cancer diagnostics. Histopathology. 2014;64(2):293-305.

75. Kim S-W, Roh J, Park C-S. Immunohistochemistry for Pathologists: Protocols, Pitfalls, and Tips. Journal of Pathology and Translational Medicine. 2016;50(6):411-8.

76. Katikireddy KR, O'Sullivan F. Immunohistochemical and immunofluorescence procedures for protein analysis. Methods in molecular biology (Clifton, NJ). 2011;784:155-67.

77. Renshaw S. Chapter 4.2 - Immunohistochemistry and Immunocytochemistry. In: Wild D, editor. The Immunoassay Handbook (Fourth Edition). Oxford: Elsevier; 2013. p. 357-77.

78. Rikardsen OG, Bjerkli I-H, Uhlin-Hansen L, Hadler-Olsen E, Steigen SE. Clinicopathological characteristics of oral squamous cell carcinoma in Northern Norway: a retrospective study. BMC Oral Health. 2014;14(1):103.

79. Rikardsen OG, Magnussen SN, Svineng G, Hadler-Olsen E, Uhlin-Hansen L, Steigen SE. Plectin as a prognostic marker in non-metastatic oral squamous cell carcinoma. BMC Oral Health. 2015;15(1):98.

80. Slaoui M, Fiette L. Histopathology Procedures: From Tissue Sampling to Histopathological Evaluation. In: Gautier J-C, editor. Drug Safety Evaluation: Methods and Protocols. Totowa, NJ: Humana Press; 2011. p. 69-82.

81. Molina-Privado I, Jiménez-P R, Montes-Moreno S, Chiodo Y, Rodríguez-Martínez M, Sánchez-Verde L, et al. E2F4 plays a key role in Burkitt lymphoma tumorigenesis. Leukemia. 2012;26(10):2277-85.

82. Ginsberg D, Vairo G, Chittenden T, Xiao ZX, Xu G, Wydner KL, et al. E2F-4, a new member of the E2F transcription factor family, interacts with p107. Genes & development. 1994;8(22):2665-79.

83. Dhanasekaran K, Bose A, Rao VJ, Boopathi R, Shankar SR, Rao VK, et al. Unraveling the role of aurora A beyond centrosomes and spindle assembly: implications in muscle differentiation. FASEB journal : official publication of the Federation of American Societies for Experimental Biology. 2019;33(1):219-30.

84. Li LL, Xue AM, Li BX, Shen YW, Li YH, Luo CL, et al. JMJD2A contributes to breast cancer progression through transcriptional repression of the tumor suppressor ARHI. Breast cancer research : BCR. 2014;16(3):R56.

85. Xu W, Yan Z, Hu F, Wei W, Yang C, Sun Z. Long non-coding RNA GAS5 accelerates oxidative stress in melanoma cells by rescuing EZH2-mediated CDKN1C downregulation. Cancer cell international. 2020;20:116.

86. Mark KMK, Varn FS, Ung MH, Qian F, Cheng C. The E2F4 prognostic signature predicts pathological response to neoadjuvant chemotherapy in breast cancer patients. BMC Cancer. 2017;17:306.

87. Paquin M, Rivard N. E2F4 (E2F transcription factor 4, p107/p130-binding). 2012.

88. Jung Y-D, Cho JH, Park S, Kang M, Park S-J, Choi DH, et al. Lactate Activates the E2F Pathway to Promote Cell Motility by Up-Regulating Microtubule Modulating Genes. Cancers (Basel). 2019;11(3):274.

89. Gaubatz S, Lees JA, Lindeman GJ, Livingston DM. E2F4 is exported from the nucleus in a CRM1-dependent manner. Molecular and cellular biology. 2001;21(4):1384-92.

90. Grimm M. Prognostic value of clinicopathological parameters and outcome in 484 patients with oral squamous cell carcinoma: microvascular invasion (V+) is an independent prognostic factor for OSCC. Clinical and Translational Oncology. 2012;14(11):870-80.

91. Cheng C, Lou S, Andrews EH, Ung MH, Varn FS. Integrative Genomic Analyses Yields Cell Cycle Regulatory Programs with Prognostic Value. Molecular cancer research : MCR. 2016;14(4):332-43.

92. Khaleel SS, Andrews EH, Ung M, DiRenzo J, Cheng C. E2F4 regulatory program predicts patient survival prognosis in breast cancer. Breast cancer research : BCR. 2014;16:486.

93. Feng Y, Li L, Du Y, Peng X, Chen F. E2F4 functions as a tumour suppressor in acute myeloid leukaemia via inhibition of the MAPK signalling pathway by binding to EZH2. Journal of Cellular and Molecular Medicine. 2020;24(3):2157-68.

94. Vaidyanathan S, Thangavelu PU, Duijf PH. Overexpression of Ran GTPase Components Regulating Nuclear Export, but not Mitotic Spindle Assembly, Marks Chromosome Instability and Poor Prognosis in Breast Cancer. Targeted oncology. 2016;11(5):677-86.

95. Viglietto G, Motti ML, Bruni P, Melillo RM, D'Alessio A, Califano D, et al. Cytoplasmic relocalization and inhibition of the cyclin-dependent kinase inhibitor p27Kip1 by PKB/Akt-mediated phosphorylation in breast cancer. Nature Medicine. 2002;8(10):1136-44.

96. Teng Y, Hu L, Yu B, Li X, Chen M, Fu X, et al. Cytoplasmic p27 is a novel prognostic biomarker and oncogenic protein for nasopharyngeal carcinoma. Artificial Cells, Nanomedicine, and Biotechnology. 2020;48(1):336-44.

97. Kau TR, Way JC, Silver PA. Nuclear transport and cancer: from mechanism to intervention. Nature reviews Cancer. 2004;4(2):106-17.

98. Cheng C, Lou S, Andrews EH, Ung MH, Varn FS. Integrative Genomic Analyses Yield Cell-Cycle Regulatory Programs with Prognostic Value. Molecular cancer research : MCR. 2016;14(4):332-43.

99. Khuu C, Utheim TP, Sehic A. The Three Paralogous MicroRNA Clusters in Development and Disease, miR-17-92, miR-106a-363, and miR-106b-25. Scientifica (Cairo). 2016;2016:1379643-.

100. Lin Y, Xu T, Zhou S, Cui M. MicroRNA-363 inhibits ovarian cancer progression by inhibiting NOB1. Oncotarget. 2017;8(60):101649-58.

101. Valencia-Sanchez MA, Liu J, Hannon GJ, Parker R. Control of translation and mRNA degradation by miRNAs and siRNAs. Genes & development. 2006;20(5):515-24.

102. Behm-Ansmant I, Rehwinkel J, Izaurralde E. MicroRNAs silence gene expression by repressing protein expression and/or by promoting mRNA decay. Cold Spring Harbor symposia on quantitative biology. 2006;71:523-30.

APPENDIX

APPENDIX I – OVERVIEW OF THE MATERIALS USED IN THE STUDY

Table 1: Reagents, apparatuses and kits used for the different analyses implemented in the study. *Product details, related applications and manufacturers.*

NAME	PRODUCT NUMBER	PRODUCER	RELATED APPLICATIONS
Allstars Ccrambled (Negative Control)	-	QIAGEN GmbH - Germany	Transfection
Bioruptor Plus Sonication System	-	Diagenode - Belgium/USA	Cell Lysis
Biotinylated Protien Ladder - Detection Pack	CAT# 7727	Cell Signaling Technology - Norway	Western Blot (WB)
Bovine Serum Albumin (BSA) - 2 mg/mL	LOT# 23209	Pierce by Thermo Fisher Scientific - USA	Protien Quantificition
Cell Culture Flasks	-	Falcon by Life Sciences - USA	Cell Culturing
Cells Scraper	-	Thermo Fisher Scientific - Mexico	Cell Harvesting
Chemiluminescence Peroxidase Substrate-3 (CPS-3)	C7364	Sigma Life Science by Sigma-Aldrich - USA	Western Blot (WB)
Countess II FL Automated Cell Counter	CAT# AMQAX1000	Countess by Thermo Fisher Scientific/Invitrogen - Oregon - USA	Cell Counting
Countess Cell Counting Chamber Slides	CAT# C10228	Countess by Thermo Fisher Scientific/Invitrogen - Oregon - USA	Countess II FL Automated Cell Counter
DC Protein Assay Kit	-	Bio-Rad Laboratories by Life Science Group - USA	Protein Quantificition
DAKO EnVision+ System-HPR (Diaminobenzidine - DAB) Kit	REF# K4011	DAKO Aligent - North America - USA	IHC Visualization
Dimethyl Sulfoxide (DMSO)	D8418	Sigma Life Science by Sigma-Aldrich - USA	Cryopreservation
DPX Mountant	-	Sigma Life Science by Sigma-Aldrich - USA	Mounting - IHC
Dithiothreitol (DTT) - 3M	-	-	Western Blot (WB)
Dulbecco's Modified Eagle's Medium (DMEM) - High Glucose	D5796	Sigma Life Science by Sigma-Aldrich - UK	Cell Culturing
Dulbecco's Phosphate Buffer Saline (DPBS)	D5773	Merck Millipore - Germany	-
Ethanol	CAT# 32221	Sigma Life Science by Sigma-Aldrich - USA	-
E.Z.N.A. HP Total RNA Kit	200	Omega BIO-TEK - USA	RNA Extraction
FastStart Essential DNA Green Master	REF# 06924204001	Roche Diagnostics GmbH - Germany	RT-qPCR

Fetal Bovine Serum (FBS)	F7524	Sigma Life Science by Sigma-Aldrich - USA	Cell Culturing
Glycine	M103	VWR Chemicals - USA	Western Blot (WB)
Goat Serum (GS)	REF# X0907	Dako - Denmark	IHC
ImageQuant LAS 4000	-	GE Healthcare Bio-Sciences AB - Sweden	Digital imaging - WB
Immobilon-P Polyvinylidene FLuoride (PDVF) Membrane	CAT# IPVH00010	Merck Millipore - USA	Western Blot (WB)
INTERFERin - siRNA Transfection Reagent	CAT# 40905	Polyplus Transfection, Illkirch, France	Transfection
LightCycler 96 Instrument	-	Roche Molecular Systems - USA	RT-qPCR
Methanol	CAT# 20847318 LOT#19G024007	VWR Chemicals - USA	Western Blot (WB)
Milli-Q Water	-	-	-
miR-363-5p mimic	-	GenePharma - China	Transfection
NanoDrop 2000 Spectrophotometer	-	Thermo Fisher Scientific - USA	RNA Quantification
NE-PER™ Nuclear and Cytoplasmic Extraction Reagents	78833	NE-PER by Thermo Fisher Scientific - USA	Cell Fractionation
NUPAGE 4-12% Bis-Tris, 1.0 mm, Mini Protein Gel, 12-well	NP0322BOX	Novex/NuPAGE by Thermo Fisher Scientific/Invitrogen - UK	Gel Elecrtrophoresis - WB
NuPAGE MES SDS Running Buffer (20X)	NP0002 LOT#2010994	NuPAGE by Thermo Fisher Scientific/Invitrogen - UK	Western Blot (WB)
Protease Inhibitor	CAT# P8340	Sigma Life Science by Sigma-Aldrich - UK	Cell Lysis
QuantiTect Reverse Transcription Kit	REF# 205314	QIAGEN GmbH - Germany	cDNA Synthesis & gDNA Wipeout - RT-qPCR
Re-Blot Plus Mild Solution (10X)	CAT# 2502	Merck Millipore - USA	Western Blot (WB)
SeeBlue Pre-Stained Protein Standard	LC5625	Thermo Fisher Scientific/Invitrogen - USA	Western Blot (WB)
Sodium Chloride (NaCl)	CAT# 27810295 LOT# 17H104108	VWR Chemicals - USA	-
Tris (Hyrdroxymethyl) Aminomethane (TRIS Base)	28811295	VWR Chemicals - USA	Western Blot (WB)
Trypan Blue (0.4%)	-	Sigma Life Science by Sigma-Aldrich - USA	Cell Counting
Trypsin-EDTA Solution (0.5 g/l porcine trypsin and 0.2g/l EDTA)	T3924	Sigma Life Science by Sigma-Aldrich - USA	Cell Culturing
VERSAmax PLUS Microplate Reader	-	Molecular Devices - California -USA	Protein Quantificition
VS120 Virtual Slide Microscope	-	Olympus Life Science Solutions - USA	Digital imaging - IHC
XCell SureLock Mini-Cell Electrophoresis System	-	Thermo Fisher Scientific/Invitrogen - UK	Gel Electrophoresis - WB

APPENDIX II – OVERVIEW OF THE BUFFERS USED IN THE STUDY

Table 2: Buffers used for the different analyses implemented in the study. *Composition of buffers and their related application.*

BUFFER	COMPOSITION	RELATED APPLICATIONS
Blotting Buffer -1L	- Tris (base; MW: 121.14 g/mol) - 5.7 g - Glycine (MW: 75.067 g/mol) - 29 g - Methanol - 200 mL - Milli-Q Water - 800 mL	WB
NuPAGE Running Buffer - 600 mL	- NuPAGE MES SDS Running Buffer (20x) - 30 mL - Milli-Q Water - 570 mL	Gel Electrophoresis - WB
1X TBST (Tris-Buffered Saline Solution with Tween) - 1L	- 5M NaCl - 30 mL - 1M Tris pH 8.0 - 20 mL - 100% Tween 20 - 20 mL - Milli-Q water - 950 mL	WB
5X Loading Buffers - 25 mL	- 0.25M Tris-HCl pH 6.8 - 6.25 mL - Sucrose - 5g - 20% SDS - 12.5 mL - Bromophenol blue - 0.05 g - Milli-Q water - 7 mL	Gel Electrophoresis - WB
RIPA Buffer - 200 mL	- Tris-HCl, pH 7.6 - 0.06 g - Triton X-100 - 2 g - Sodium Chloride - 0.03 ml - Sodium dodecyl sulfate (SDS) - 0.2 g - Na-deoxycholate - 1g	Cell Lysis
1X Phosphate Buffer Saline - 5L	- Phosphate buffer saline (9.55 g/L) - 47.75g - Milli-Q-water - 5 L	Cell Culturing, WB and IHC

APPENDIX III – OVERVIEW OF THE ANTIBODIES USED IN THE STUDY

Table 3: Monoclonal and polyclonal antibodies used for the different analyses implemented in the study. *Product details, related applications and manufacturers.*

ANTIBODY	TRAGET	HOST	CONJUGATE	PRODUCT NUMBER	PRODUCER	RELATED APPLICATIONS
Anti-E2F4 - monoclonal - IgG	Human E2F4	Rabbit	-	[EPR8259] (ab150360)	Abcam - Cambridge - UK	WB and IHC
Anti-Rabbit - Polyclonal - IgG	Rabbit	Goat	Horse Radish Peroxidase (HPR)	CAT# 405005	SouthernBiotech - USA	WB and IHC
Anti-Lamin B1 - Polyclonal - IgG	Human Lamin B1	Rabbit	-	(ab16048)	Abcam - Cambridge - UK	Loading Control - WB
Anti-Vinculin - Polyclonal - IgG	Human vinculin	Rabbit	-	CAT# V4139	Sigma-Aldrich - USA	Loading Control - WB
Anti-Biotin	-	Goat	Horse Radish Peroxidase (HPR)	CAT# 7075P5	Cell Signaling Technology - Norway	Ladder Detection - WB

APPENDIX IV – OVERVIEW OF THE PRIMERS USED IN THE STUDY

Table 4: Primers used to execute the RT-qPCR procedure in the study. *All primers were from the same producer Sigma-Aldrich, USA. Gene names, GenBank accession numbers, primer sequences (F: Forward and R: Reverse), size and PCR efficiency of reference and target RNAs.*

GENE	FULL NAME	ACCESSION NUMBER	PRIMER SEQUENCE (5' - 3')	SIZE (bp)	PCR EFFICIENCY/R2
Hs_ActB (Reference gene)	Homo Sapiens Acin Beta, mRNA	NM001101.3	F: TCCTCACCCTGAAGTACCCCA R: AGCCACACGCAGCTCATTGTA	100	100/0.999
Hs_eF1a (Reference gene)	Homo Sapiens Eukaryotic Translation Elongation Factor 1 Alpha 1(EEF1A1), mRNA	NM001402.5	F: GTTCCTGGCAAGCCCATGT R: TGATGACACCCACCGCAAC	102	95.2/0.999
Hs_B2M (Reference gene)	Homo Sapiens Beta-2-Microglobulin, mRNA	NM004048.2	F:TGTCTTTCAGCAAGGACTGGTCT R:GACAAAGTCACATGGTTCACACG	102	96.6/0.999
Hs_E2F4 (Target gene)	Homo Sapiens E2F Transcription Factor 4, mRNA	NM001950.3	F: CCAGGAAGCCTCACGTCCA R: ACTGTGATCTCAGCTGCTGGG	101	97.9/0.999